IEEE Access
Multidisciplinary ⋮ Rapid Review ⋮ Open Access Journal

Received 27 April 2024, accepted 14 May 2024, date of publication 17 May 2024, date of current version 24 May 2024.

Digital Object Identifier 10.1109/ACCESS.2024.3402318

RESEARCH ARTICLE

Dynamic Spectrum Sharing in a Blockchain Enabled Network With Multiple Cell-Free Massive MIMO Virtual Operators

GUILLEM FEMENIAS[1], (Senior Member, IEEE), M. FRANCISCA HINAREJOS[2], FELIP RIERA-PALOU[1], (Senior Member, IEEE), JOSEP-LLUIS FERRER-GOMILA[2], AND AMADOR JAUME-BARCELÓ[2]

[1]Mobile Communications Group (MCG), Balearic Institute for Artificial Intelligence Research (IAIB), University of the Balearic Islands (UIB), 07122 Palma, Spain
[2]Security and Electronic Commerce Group (SECOM), UIB, 07122 Palma, Spain

Corresponding author: Guillem Femenias (guillem.femenias@uib.es)

We acknowledge support from grants IRENE-STARMAN (PID2020-115323RB-C32 funded by MCIU/AEI/10.13039/501100011033, Spain), GERMINAL (TED2021-131624B-I00, funded by MCIU/AEI/10.13039/501100011033, Spain, and by European Union "NextGenerationEU"/PRTR), and BLOBSEC (PID2021-122394OB-I00, funded by MCIU/AEI/10.13039/501100011033, Spain, and by ERDF A way of making Europe).

ABSTRACT This paper introduces a novel dynamic spectrum sharing (DSS) scheme designed for cell-free massive MIMO (CF-mMIMO) networks. The motivation behind this work arises from the urgent need to enhance spectrum utilization in modern wireless communication systems. Traditional spectrum allocation methods often struggle to meet the diverse spectrum demands of different wireless operators. The proposed approach addresses these challenges by enabling the spectrum provider (SP) to flexibly allocate and sell its spectrum resources, empowering wireless virtual operators to acquire bandwidth efficiently based on their specific needs. In our framework, each wireless operator is represented by a CF-mMIMO network, characterized by an average spectral efficiency metric that quantifies the potential value of additional spectrum acquisition. Leveraging a Stackelberg game formulation, our DSS policy achieves an equilibrium point that optimally allocates bandwidths to operators and determines corresponding prices. This approach not only enhances spectrum utilization but also fosters fair competition among operators. A key innovation of our work lies in the utilization of blockchain technology, where all spectrum transactions are managed through a smart contract. This ensures transparency, integrity, and auditability throughout the spectrum trading process. The novel protocol facilitates seamless information exchange, orchestrates the Stackelberg game dynamics, and delivers conclusive outcomes to both the SP and the CF-mMIMO operators.

INDEX TERMS Cell-free massive MIMO, blockchain, Stackelberg game, dynamic spectrum sharing, smart contract.

I. INTRODUCTION

A. CONTEXT AND MOTIVATION

The development of sixth generation (6G) wireless networks is poised to revolutionize the way we connect and communicate [1]. However, this next-generation wireless technology brings with it a set of formidable challenges that must be confronted. Meeting the demands of ultra-high data rates, ultra-low latency, energy efficiency, and ubiquitous connectivity, while addressing privacy and cybersecurity concerns, represents a daunting task, especially in the context of an increasingly congested frequency spectrum [2], [3]. 6G networks will require groundbreaking innovations in spectrum management and infrastructure deployment to realize the vision of a seamlessly connected and intelligent future.

One of the technologies frequently cited as a pillar underpinning the future generation of mobile communications is the cell-free massive MIMO (CF-mMIMO) architecture. CF-mMIMO networks, which have been introduced in [4],

The associate editor coordinating the review of this manuscript and approving it for publication was Walid Al-Hussaibi.

[5], and [6], are a novel paradigm aiming at providing uniform high quality of service (QoS) metrics for every mobile station (MS) across a large geographical area. Towards this end, many access points (APs) are deployed across an entire coverage area and they are all connected through fronthaul links to a central processing unit (CPU) who is in charge of the signal processing required to cooperatively serve all MSs using the same frequency/time resources. Indeed, the CF-mMIMO concept can be seen as the combination of two trends already present in current networks, namely, ultradensification and massive multiple-input multiple-output (MIMO) [7]. The last few years have witnessed the development of the theoretical basis underpinning CF-mMIMO networks, covering aspects such as combiner and precoder design, power and pilot allocation or the use of imperfect fronthauls. While this theory heavily relies on the same principles as cellular massive MIMO systems, there are also important differences caused by the distributed nature of the antenna array deployment. Readers are referred to [8] for a comprehensive treatment of the main results in CF-mMIMO networks.

When there are several CF-mMIMO networks in a given coverage area, each one owned by a different network operator, spectrum management may play a key role in efficiently managing radio resources, specially in scenarios where wildly different frequency bands are operational as it is envisioned in 6G ecosystems [9]. In conventional systems, each network infrastructure serves its users with the spectrum resources assigned by a radio spectrum regulator in a fixed and a-priori manner, ensuring that the bandwidths assigned to different networks do not overlap. This static frequency allocation, however, may lead to a poor spectrum usage if some of the networks have a surplus of bandwidth allocated while others require of more radio resources to provide service. Spectrum management is expected to become even more critical in 6G given a context of rate-hungry applications such as augmented reality or autonomous driving, that may need to co-exist with other user requirements such as massive sensor connectivity [10]. Consequently, a more flexible and efficient spectrum management that increases spectrum efficiency and reduces underutilized spectrum is appealing [11]. The concept of mobile virtual network operators (MVNOs) became popular during the roll-out of the fourth generation (4G) of mobile networks [12]. An MVNO is an entity that does not own either telecom network infrastructure or assigned frequency bands (or neither of them) but provides telecom services by purchasing capacity from (conventional) mobile network operators (MNOs) or/and central spectrum providers (SPs). In this work focus is put on the case where these MVNOs do own network infrastructure but they lack frequency spectrum and hence they must purchase it to an SP. In this case, the implementation of dynamic spectrum sharing (DSS) could improve spectrum utilization rates by allowing the SP to dynamically allocate spectrum to virtual operators that are willing to buy all or part of this spectrum [13]. This technique has been known to offer substantial spectral efficiency gains in comparison to static spectrum assignment [14]. The dynamic assignment of spectrum may be executed frequently, either periodically or when network parameters change significantly [15], and often implies solving optimization problems. Very early on, game theory was recognized as a useful analytical tool to guide the competition among different operators/SPs to efficiently manage the spectrum while maximizing a prescribed utility function [16], [17].

Whatever the game model adopted, the process must conclude with a compromise between the SP and the network operators: the owner will provide spectrum resources to the operators, and the operators will pay the owner for the use of the allocated spectrum resources. That is, these actors must sign a contract. Therefore, a contract signing protocol must be designed to guarantee the security of the process. The fundamental security requirement to be met is fairness [18], [19], [20], [21]: either both signatories have evidence of the other signatory's commitment, or neither of them has such evidence. In other words, none of the signatories should be left at a disadvantage as a result of the execution of the contract signing protocol.

Traditionally, the fairness requirement has been achieved by designing contract signing protocols that rely on the existence and possible intervention of a trusted third party (TTP) [20], [22], [23], [24]. If one of the signatories observes that at any time during the execution of the contract signing protocol he is at a disadvantage, he must request the intervention of the TTP to restore the fairness of the exchange. However, it can be difficult for the parties to agree on a TTP that is trustworthy for all signatories. Furthermore, the TTP becomes a possible point of failure (for example, if the TTP goes out of service or if the TTP is dishonest). The substitution of TTPs for the use of the blockchain has been witnessed recently [25], [26], [27], [28], [29], [30]. The blockchain is a distributed, immutable and transparent registry that, when combined with the feature of executing immutable code in the form of smart contracts (SCs), could be used to implement a DSS system complying with the fairness requirement.

B. PREVIOUS RESEARCH WORK

A few works have designed and implemented solutions that use DSS in conjunction with blockchain technology to facilitate ledger operations. Han and Zhu [31] introduce a permissioned blockchain implementation of a spectrum sharing algorithm rooted in game theory to identify a Nash equilibrium point, leveraging the Ethereum blockchain for economic transactions. However, the negotiation process among spectrum operators lacks clarity on key aspects. For instance, according to the authors, only the spectrum provider broadcasts a transaction on the blockchain with the negotiation outcome, prompting concerns regarding fairness due to the lack of evidence regarding the consenting agreement from the requesting operator concerning spectrum

TABLE 1. List of main acronyms (in alphabetical order).

Acronym	Description
5G	Fifth generation
6G	Sixth generation
AP	Access point
CF-mMIMO	Cell-free massive MIMO
CPU	Central processing unit
DCC	Dynamic cooperation clustering
DL	Downlink
DSS	Dynamic spectrum sharing
EVM	Ethereum virtual machine
KKT	Karush-Kuhn-Tucker
MIMO	Multiple-input multiple-output
MMSE	Minimum mean square error
MNO	Mobile network operator
MS	Mobile station
MVNO	Mobile virtual network operator
QoS	Quality of service
SC	Smart contract
SINR	Signal-to-interference-plus-noise ratio
SP	Spectrum provider
TDD	Time division duplex
TTP	Trusted third party
UL	Uplink

allocation and pricing. Alhosani et al. [32] describe a spectrum auction in Ethereum that periodically executes the following three phases: the registration of entities as sellers or buyers of spectrum resources, the spectrum allocation phase in which an offer from a spectrum buyer is matched to an offer from a spectrum seller and, finally, the payment step from buyers to sellers. The authors of this paper provide the cost of executing each function, but they neither offer a detailed analysis of the cost in a fiat currency nor study its evolution over time. Lin et al. [33] define a scenario in which primary users who own spectrum resources can sell them to secondary users who demand these resources and propose a theoretical non-cooperative game based on utility functions to allocate the spectrum resources. This proposal, however, does not provide any information regarding the commitment process between the intervening actors. Li et al. [34] consider multiple spectrum sellers and multiple spectrum buyers and present a consortium blockchain-based DSS proposal. This work, however, does not realistically model the spectral efficiencies of the mobile networks taking part in the game. Indeed, the lack of a realistic model for the physical layer is a rather prevalent limitation in most prior research works (e.g., [31], [32], [33]). Qiu et al. in [35] implement a secure spectrum trading framework using a consortium blockchain for unmanned aerial vehicle (UAV)-assisted cellular networks, enabling mobile network operators (MNOs) and UAV operators to trade spectrum without relying on a TTP. Similar to our proposal, utility functions for both MNOs and unmanned aerial vehicle (UAV) operators are optimized using a Stackelberg game model while exploring nonuniform and uniform pricing schemes. Similar to many previously cited references, however, this work does not include a detailed analysis of the costs associated with implementing the blockchain-based protocol in a fiat currency, nor does it study its evolution over time.

It is interesting to note that the formulation of Stackelberg games aimed at maximizing the utility functions of providers of different types of services and the operators of these services in scenarios where a blockchain is used to ensure transaction security and privacy, is a widely used solution in research contexts substantially different from the one addressed in our research work. Just to name a few examples, Jiang et al. in [36] develop a multi-leader multi-follower Stackelberg game to address the computing resource management problem in a mobile blockchain mining scenario. Xu et al. in [37] design a consortium blockchain-based data trading framework in a car-sharing data market, where a three-layer Stackelberg game (involving data owners, service providers, and data buyers) is formulated and analyzed.

C. MAIN AIM AND CONTRIBUTIONS

This paper is the first to explore spectrum sharing policies in the context of cell-free networks subject to the restriction that the outcomes of the spectrum trade should be accountable. The policy governing how different operators share the spectrum is significantly shaped by the spectral efficiencies that each network can provide to its subscribers. Logically, this efficiency is closely linked to the fees charged to subscribers for accessing the network services. As expected, the better the spectral efficiency, the more value subscribers perceive in the service, potentially justifying higher subscription fees. The introduction of blockchain technology to securely record spectrum transactions adds another layer of complexity and cost to the spectrum sharing process that impacts both operators and spectrum regulators while guaranteeing the integrity and transparency of spectrum trading activities. Therefore, when evaluating the benefits and economic implications of spectrum sharing, it is crucial to jointly consider both the spectral efficiency of networks and the costs associated with the use of blockchain technology to fully grasp the trade-offs involved in spectrum sharing arrangements. Specifically, key questions arise: What are the benefits of spectrum sharing in a 6G context, such as that envisaged for cell-free networks? Can this spectrum sharing be administered in a fair and accountable manner? What are the costs and penalties associated with such a spectrum management strategy? This paper aims to provide precise answers to these questions while addressing many of the shortcomings identified in previous research. In particular, it introduces a DSS specifically targeting CF-mMIMO, a promising 6G topology, and proposes the use of a blockchain to manage, on the one hand, the spectrum trade through the use of

a SC and, on the other hand, the storage of the required information. Based on the established facts of current and expected spectrum shortage and the consolidation of CF-mMIMO as one of the pillars of 6G, we hypothesize that blockchain-backed spectrum sharing can be a key mechanism towards optimizing its usage in an accountable manner. Once the problem is formalized, Stackelberg game theory is able to provide the optimal solution and the results of the game governing the spectrum trade can be effectively registered on the blockchain. Numerical results have confirmed the validity of our approach. In more detail, the main contributions of this paper are:

- The problem of spectrum allocation is formulated as a game in which the SP tries to maximize the revenue resulting from the sale of the spectrum it owns while the different network operators try to maximize a spectral-efficiency related utility function that increases with the assigned bandwidth but simultaneously factors in the cost of the acquired spectrum. The resulting optimization problem is revealed to be a Stackelberg game, which allows for a closed-form solution. This solution provides the optimal bandwidth assignments to each operator, along with their respective prices.
- Remarkably, the spectral efficiencies (SEs) feeding the Stackelberg game are the result of a physical layer abstraction of CF-mMIMO networks that allows to assess the effects different infrastructure parameters (i.e., the number of APs, the number of antennas at the APs or the network load) have on the game solution.
- All the input parameters to the game (i.e., bandwidth available at the SP, SEs) and the resulting outcomes (i.e., allocated bandwidths and prices) are recorded onto a blockchain that guarantees the integrity and auditability of the spectrum allocation process. Towards this end, all the required operations interfacing with the blockchain are specified and formalized in the form of a blockchain-aided DSS protocol.
- The deployment of the SC has been conducted onto different blockchains, namely, Ethereum and Polygon. This implementation allows a realistic evaluation of the cost and delay that the use of the blockchain brings along.

D. ORGANIZATION OF THE PAPER

The remainder of this paper is organized as follows. Section II describes the CF-mMIMO model considered in this scenario and the relation between the different network entities and the blockchain infrastructure. The formulation of the Stackelberg game for allocating bandwidth to each operator to optimize a predefined utility function is defined in Section III. The algorithm to solve the Stackelberg game is presented in Section IV. Section V introduces the blockchain features and required protocol to implement the DSS scheme. Section VI presents the numerical results analysis of the Stackelberg game as a function of different network parameters. Furthermore, results derived from the implementation of the DSS protocol using Ethereum and Polygon blockchains are presented. Lastly, Section VII provides a summary of the conclusions and offers guidance for future work. For ease of reference, the most important acronyms and related descriptions are reproduced in Table 1.

This introduction concludes with a brief notational remark: scalars, vectors and matrices are denoted by lower-case non-bold, lower-case bold and upper-case bold characters, respectively. $\text{diag}\,(\boldsymbol{X}_1, \ldots, \boldsymbol{X}_n)$ is used to denote a block diagonal matrix comprising matrices $\boldsymbol{X}_1, \ldots, \boldsymbol{X}_n$ on its main block diagonal. The trace of a matrix $\boldsymbol{X}$ is denoted by $tr(\boldsymbol{X})$. $\mathcal{CN}(\boldsymbol{m}, \boldsymbol{R})$ denotes a circularly symmetric complex Gaussian vector distributions with mean $\boldsymbol{m}$ and covariance $\boldsymbol{R}$. Superscripts ^{H} and ^{T} serve to denote Hermitian and transpose, respectively, of the variable where they are applied.

II. SYSTEM MODEL

A. GENERAL SYSTEM MODEL

As shown in Fig. 1, a DSS scenario is considered where the SP, owning a total bandwidth B, provides chunks of bandwidth to C virtual CF-mMIMO operators. The chunk of bandwidth allocated to the cth operator is denoted as B_c, and p_c denotes the price per unit of bandwidth paid by the operator to the SP. The cth CF-mMIMO network consists of M_c geographically distributed APs, each equipped with an array of N_c antennas, cooperating to jointly serve, on the same time-frequency resources, K_c single-antenna MSs, and resulting in an aggregate spectral efficiency (meausured in bit/s/Hz), which is denoted as η_c. All APs in a particular CF-mMIMO network are assumed to be connected to a CPU (or a group of CPUs) via error-free infinite capacity fronthaul links. It is assumed here that the network operates at a sub-6 GHz carrier frequency, thus allowing the use of propagation and system models that have been widely employed in the recent cell-free literature (see for instance [8] and references therein).

The chunks of bandwidth to be allocated to each of the virtual CF-mMIMO operators and the prices they have to pay to the SP are determined through a competitive game aiming at optimizing predetermined utility-related functions. These utility functions are related, on the one hand, to the revenue that the SP will obtain from the sale of the bandwidth, and on the other hand, to the benefits (in terms of QoS) that each of the operators can derive from the service they provide to the associated MSs. In order to ensure that all transactions between the spectrum provider and operators comply with prescribed security requirements, the entire process is carried out through a smart contract SC deployed on the blockchain. Specifically, the SP communicates the available bandwidth to the smart contract while the CF-mMIMO operators, in turn, communicate the spectral efficiencies they can provide. Using this data, and taking into account the utility functions to be optimized, the SC implementing the DSS algorithm is executed to determine the optimal chunks of bandwidth to

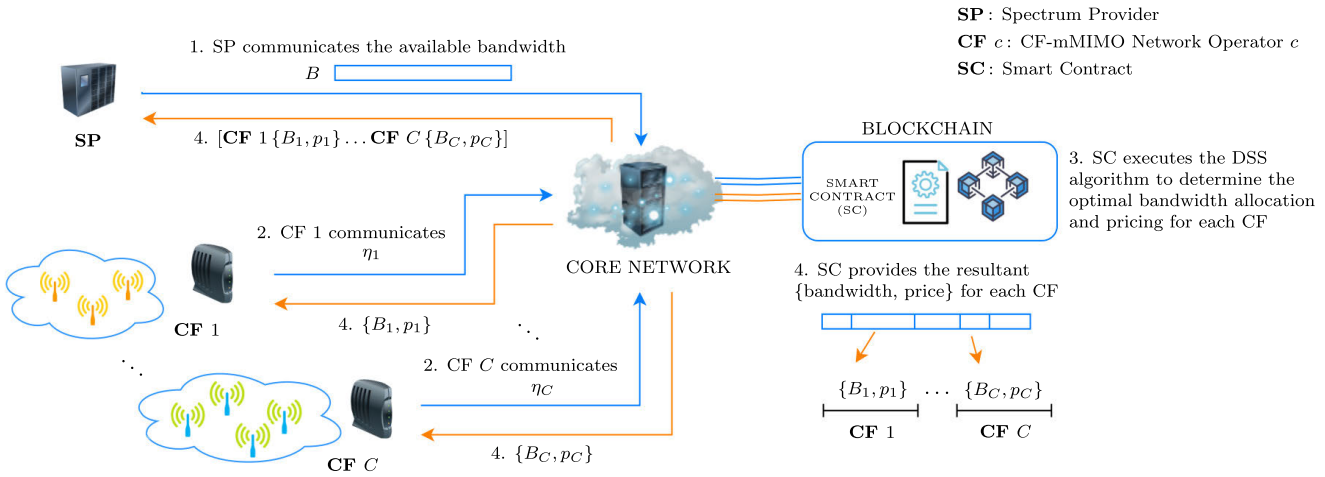

FIGURE 1. System model depicting the main entities and variables used in this work. Numbering labels represent the steps taken by the proposed scheme that will be detailed in Section V.

be assigned to the CF-mMIMO operators and the prices they have to pay to the SP. Therefore, all the information involved in the DSS process is recorded transparently and auditably on the blockchain.

Before delving into the details of our proposal, and for the readers unfamiliar with any of the three main techniques involved in this work, we refer to [38], [39], and [40], as tutorial introductions to the topics of cell-free networks, game theory in wireless communications and blockchain technology, respectively.

B. MODELING THE SPECTRAL EFFICIENCY

Propagation channels among APs and MSs are characterized by, on the one hand, small-scale fading parameters that can be assumed to be static within a time-frequency interval referred to as the *coherence interval* and, on the other hand, large-scale parameters (i.e., spatial correlation matrices including the large-scale propagation gains) that can be considered to be static over many coherence intervals (typically tens or even hundreds in low-mobility scenarios) and that are potentially known a-priori at each AP in the corresponding network [41], [42], [43], [44]. The channel between the MS k and the mth AP of the cth CF-mMIMO network is assumed to be distributed as $\boldsymbol{h}_{cmk} \sim \mathcal{CN}(\boldsymbol{0}, \boldsymbol{R}_{cmk})$ where $\boldsymbol{R}_{cmk} \in \mathbb{C}^{N_c \times N_c}$ is the spatial correlation matrix. In this case, the small-scale fading is modeled by the Gaussian distribution whereas the large-scale fading is described by the spatial correlation matrix, with $\beta_{cmk} = \text{tr}(\boldsymbol{R}_{cmk})/N_c$ representing the joint effects of path-loss, shadowing and antenna gains. The channel vectors between a particular MS and different APs are assumed to be independently distributed and, hence, the collective channel $\boldsymbol{h}_{ck} = \left[\boldsymbol{h}_{c1k}^T \ldots \boldsymbol{h}_{cM_ck}^T\right]^T$ between MS k all the APs conforming the cth CF-mMIMO network is distributed as $\boldsymbol{h}_{ck} \sim \mathcal{CN}(\boldsymbol{0}, \boldsymbol{R}_{ck})$, where $\boldsymbol{R}_{ck} = \text{diag}\left(\boldsymbol{R}_{c1k}, \ldots, \boldsymbol{R}_{cM_ck}\right)$ is the block-diagonal collective spatial correlation matrix.

In each of the CF-mMIMO networks, transmissions between APs and MSs are organized in a time division duplex (TDD) operation whereby the frames, with a length of τ_{f_c} samples, for all $c \in \{1, \ldots, C\}$, are assumed to fit the coherence interval. Each TDD frame is split into three phases, namely, the uplink (UL) training phase, the UL payload data transmission phase and the downlink (DL) payload data transmission phase, whose lengths, measured in samples, are denoted as τ_{p_c}, τ_{uc} and τ_{dc}, respectively, and holding $\tau_{f_c} = \tau_{p_c} + \tau_{uc} + \tau_{dc}$. In each CF-mMIMO network, a set of τ_{p_c} mutually orthogonal pilot sequences are used during the corresponding UL training phase. These pilot sequences are allocated to MSs in a deterministic way, and there can be different MSs using the same pilot sequence. Denoting by $\mathcal{P}_{ck}$ the set of MSs using the same pilot sequence as MS k (including itself) in the cth network, the minimum mean square error (MMSE) channel estimate of $\boldsymbol{h}_{cmk}$ is obtained as [8]

$$\hat{\boldsymbol{h}}_{cmk} = \sqrt{P_p \tau_{p_c}} \boldsymbol{R}_{cmk} \boldsymbol{\Psi}_{cmk}^{-1} \boldsymbol{y}_{cmk}, \tag{1}$$

where P_p is the transmit per-pilot symbol at the MSs, $\boldsymbol{y}_{cmk}$ is the received pilot signal vector obtained after projecting the matrix of signals received at the mth AP on the pilot sequence allocated to MS k, that is,

$$\boldsymbol{y}_{cmk} = \sqrt{P_p \tau_{p_c}} \boldsymbol{h}_{cmk} + \sqrt{P_p \tau_{p_c}} \sum_{k' \in \mathcal{P}_{ck} \setminus k} \boldsymbol{h}_{cmk'} + \boldsymbol{n}_{cmk}, \tag{2}$$

with $\boldsymbol{n}_{cmk} \sim \mathcal{CN}\left(\boldsymbol{0}, \sigma_u^2 \boldsymbol{I}_{N_c}\right)$, and

$$\boldsymbol{\Psi}_{cmk} = \mathbb{E}\left\{\boldsymbol{y}_{cmk} \boldsymbol{y}_{cmk}^H\right\} = P_p \tau_{p_c} \sum_{k' \in \mathcal{P}_{ck}} \boldsymbol{R}_{cmk'} + \sigma_u^2 \boldsymbol{I}_{N_c}. \tag{3}$$

The channel estimation error $\tilde{\boldsymbol{h}}_{cmk} = \boldsymbol{h}_{cmk} - \hat{\boldsymbol{h}}_{cmk}$ is independent of the channel estimate and distributed as $\tilde{\boldsymbol{h}}_{cmk} \sim \mathcal{CN}(\boldsymbol{0}, \boldsymbol{C}_{cmk})$, where

$$\boldsymbol{C}_{cmk} = \boldsymbol{R}_{cmk} - P_p \tau_{p_c} \boldsymbol{R}_{cmk} \boldsymbol{\Psi}_{cmk}^{-1} \boldsymbol{R}_{cmk}. \tag{4}$$

Even though there exist different strategies that could be capitalized on to allocate bandwidth to the network operators and to set the prices they must satisfy to the SP, a Stackelberg game will be formulated in this paper that will be based on the spectral efficiencies that the network operators can provide to the MSs they serve. Although the Stackelberg game can be based on both UL and DL spectral efficiencies, or even a combination of both, without loss of essential generality, only the UL spectral efficiencies will be considered in this paper. Furthermore, while these spectral efficiencies could also be determined by assuming distributed or scalable centralized UL operation strategies, for the sake of brevity, a centralized UL operation will be assumed in the proposed approach. In the centralized operation scenario, an achievable spectral efficiency in the UL of MS k in the cth CF-mMIMO network (measured in bit/s/Hz) can be expressed as [8, Section 5.1]

$$\eta_{ck} = \frac{\tau_{uc}}{\tau_{f_c}} \mathbb{E}\left\{\log_2\left(1 + \text{SINR}_{ck}\right)\right\}, \tag{5}$$

where the pre-log factor τ_{uc}/τ_{f_c} is the fraction of each coherence block that is used for UL payload data transmission, the instantaneous effective signal-to-interference-plus-noise ratio (SINR) is given by equation (6), as shown at the bottom of the next page, and the expectation is with respect to the aggregate channel estimates $\hat{\boldsymbol{h}}_{ck} = \left[\hat{\boldsymbol{h}}_{c1k}^T \ldots \hat{\boldsymbol{h}}_{cM_ck}^T\right]^T$. The variable p_{ck} is the UL transmit power allocated to MS k, the vector $\boldsymbol{v}_{ck}$ represents the aggregate combining filter implemented at the M_c APs conforming the cth CF-mMIMO network, and the matrix $\boldsymbol{C}_{ck} = \text{diag}\left(\boldsymbol{C}_{c1k}, \ldots, \boldsymbol{C}_{cM_ck}\right)$. We note that various options are at hand to select $\boldsymbol{v}_{ck}$ such as, for instance, maximal ratio combining (MRC), MMSE or zero-forcing (ZF), each providing a different SINR and spectral efficiency (see [8] for more details).

III. FORMULATION OF THE STACKELBERG GAME

A Stackelberg game is a strategic interaction model in game theory where players make sequential decisions [45]. In this model, one player, known as the leader, moves first with complete knowledge of the other players' strategies. The remaining players, called followers, observe the leader's move and then make their own decisions. In a Stackelberg game, the leader's advantage lies in its ability to commit to a strategy before the followers' turn. This commitment can influence the followers' behavior as they anticipate the leader's actions and respond accordingly. On the one hand, the leader's objective is to maximize its own revenue while considering the followers' best response. On the other hand, the followers aim to maximize their own utility given the leader's chosen strategy. In this paper, the SP will be considered as the leader, and the CF-mMIMO network operators as the followers. The SP (leader) will impose a set of prices per unit of bandwidth to each of the network operators. Then, the network operators will update their strategies for acquiring bandwidth to maximize their individual utility functions based on the assigned prices.

Let us denote by $\boldsymbol{b} = [B_1 \ldots B_C]^T$ the vector of bandwidths acquired by the network operators to the SP, and by $\boldsymbol{p} = [p_1 \ldots p_C]^T$ the vector of prices per unit of bandwidth imposed by the SP to the C network operators. Under the above Stackelberg game model, the objective of the SP is to maximize the revenue obtained from selling the bandwidth to the CF-mMIMO network operators. Mathematically, the revenue of the SP can be formulated as

$$R_{\text{SP}}(\boldsymbol{b}, \boldsymbol{p}) = \boldsymbol{b}^T\boldsymbol{p}. \tag{7}$$

Note that under the Stackelberg game formulation, the bandwidth B_c sold to the cth network operator is actually a function of the price p_c. That is, the amount of bandwidth that a particular CF-mMIMO network operator is willing to purchase depends on the price imposed by the SP. As the bandwidth available at the SP is limited, the SP must determine the prices that maximize the revenue under the aggregate bandwidth constraint. That is, this optimization problem revolves around devising a strategy to maximize revenue while respecting bandwidth limitations, and it can be formally expressed as

$$PSP: \max_{\boldsymbol{p}} R_{\text{SP}}(\boldsymbol{b}, \boldsymbol{p}) \tag{8}$$

$$\text{subject to } \sum_{c=1}^{C} B_c \leq B \tag{8a}$$

$$p_c \geq 0 \quad \forall c \in \{1, \ldots, C\}. \tag{8b}$$

Considering that the CF-mMIMO network operators offer enhanced mobile broadband (eMBB) services, it is quite reasonable to assume that on the positive side of the corresponding utilities (profit) there must be a term obeying the law of diminishing returns in terms of the spectral efficiencies (measured in bit/s) they can provide to the MSs they serve. On the negative side of the utility functions (cost), there will obviously be the budget that the SP must meet in order to cover the expenses associated with the allocated bandwidth. Hence, using a logarithmic function to model the law of diminishing returns, a suitable utility function for the cth network operator can be defined as

$$U_c(B_c, p_c) = \omega_c \log\left(1 + \frac{B_c\eta_c}{\varrho_c}\right) - B_c p_c, \tag{9}$$

where $\omega_c \geq 0$, $\varrho_c > 0$ and $\eta_c = \sum_{k=1}^{K_c} \eta_{ck}$ denote the weighting coefficient (measured in currency units), the normalizing coefficient (measured in bit/s) and the aggregate spectral efficiency (measured in bit/s/Hz) of CF-mMIMO network c, respectively. The joint effects of the weighting and normalizing coefficients can effectively be used to coordinate various prioritization strategies, depending on the potential agreements established between the network operators. Analyzing the structure of the utility function, it becomes evident that, on the one hand, by increasing the acquired bandwidth, a particular CF-mMIMO network operator improves both spectral efficiency and profit. On the other hand, acquiring more bandwidth increases the cost. Consequently, network

operators require bandwidth acquisition strategies aimed at maximizing their own utilities. In fact, the problem that must be solved by the CF-mMIMO operators (followers' side) can be formulated as

$$PCFc: \max_{B_c} U_c(B_c, p_c) \tag{10}$$

$$\text{subject to } B_c \geq 0. \tag{10a}$$

Problems **PSP** and **PCFc**, for all $c \in \{1, \ldots, C\}$, form a Stackelberg game aimed at identifying the Stackelberg equilibrium point $(\boldsymbol{b}^*, \boldsymbol{p}^*)$ where both the SP and CF-mMIMO network operators lack incentives to deviate. That is, for any point $(\boldsymbol{b}, \boldsymbol{p})$ such that $\boldsymbol{b} \geq \mathbf{0}$ and $\boldsymbol{p} \geq \mathbf{0}$, the Stackelberg equilibrium point $(\boldsymbol{b}^*, \boldsymbol{p}^*)$ satisfies

$$R_{\text{SP}}(\boldsymbol{b}^*, \boldsymbol{p}^*) \geq R_{\text{SP}}(\boldsymbol{b}^*, \boldsymbol{p}), \tag{11a}$$

$$U_c(B_c^*, p_c^*) \geq U_c(B_c, p_c^*) \quad \forall c \in \{1, \ldots, C\}. \tag{11b}$$

To obtain the Stackelberg equilibrium point in the proposed Stackelberg game, the following steps can be followed: first, problem **PCFc** must be solved for a given vector $\boldsymbol{p}$ and for each $c \in \{1, \ldots, C\}$ to determine the optimal vector of bandwidths $\boldsymbol{b}^*$; then, utilizing $\boldsymbol{b}^*$, problem **PSP** can be solved to obtain the optimal vector of prices $\boldsymbol{p}^*$.

IV. SOLVING THE STACKELBERG GAME

The first and second derivatives of $U_c(B_c, p_c)$ with respect to B_c are

$$\frac{\partial U_c(B_c, p_c)}{\partial B_c} = \frac{\omega_c \eta_c}{(\varrho_c + B_c \eta_c)} - p_c, \tag{12}$$

and

$$\frac{\partial^2 U_c(B_c, p_c)}{\partial^2 B_c} = -\frac{\omega_c \eta_c^2}{(\varrho_c + B_c \eta_c)^2}, \tag{13}$$

respectively. Since the second derivative is always negative, the utility function is concave with respect to B_c and, hence, as the constraint is affine, each of the followers' games, mathematically modeled in (10), is a convex optimization problem. By solving the Karush-Kuhn-Tucker (KKT) conditions for this problem, the optimal solution for the bandwidth that must be acquired by the cth network operator is

$$B_c^* = \left(\frac{\omega_c}{p_c} - \frac{\varrho_c}{\eta_c}\right)^+, \tag{14}$$

where $x^+ = \max(0, x)$. Thus, it can be observed that if the price is too high, that is, if $p_c \geq \omega_c \eta_c / \varrho_c$, the cth CF-mMIMO network operator will not buy any portion of the bandwidth available at the SP and will be removed from the game.

Using the optimal buying strategy of the network operators, mathematically expressed in (14), the optimization problem at the SP can be reformulated as

$$PSPR: \max_{\boldsymbol{p}} \sum_{c=1}^{C} \left(\omega_c - \frac{p_c \varrho_c}{\eta_c}\right) \tag{15}$$

$$\text{subject to } \sum_{c=1}^{C} \left(\frac{\omega_c}{p_c} - \frac{\varrho_c}{\eta_c}\right) \leq B \tag{15a}$$

$$0 \leq p_c \leq \frac{\omega_c \eta_c}{\varrho_c} \quad \forall c \in \{1, \ldots, C\}. \tag{15b}$$

The main challenge in solving this optimization problem is related to constraint (15b). If this constraint is removed, problem **PSPR** is convex, satisfies Slater's condition, and allows for obtaining the optimal solution by imposing the KKT conditions. Specifically, the Lagrangian function associated with this relaxed optimization problem can be expressed as

$$\mathcal{L}(\boldsymbol{p}, \lambda) = \sum_{c=1}^{C} \left(\omega_c - \frac{p_c}{\eta_c \varrho_c}\right) + \lambda \left[B - \sum_{c=1}^{C} \left(\frac{\omega_c}{p_c} - \frac{\varrho_c}{\eta_c}\right)\right] \tag{16}$$

where $\lambda \geq 0$ is the Lagrange multiplier, and the KKT conditions can then be written as

$$\frac{\partial \mathcal{L}(\boldsymbol{p}, \lambda)}{\partial p_c} = -\frac{\varrho_c}{\eta_c} + \lambda \frac{\omega_c}{p_c^2} = 0, \tag{17a}$$

$$\lambda \left[B - \sum_{c=1}^{C} \left(\frac{\omega_c}{p_c} - \frac{\varrho_c}{\eta_c}\right)\right] = 0, \tag{17b}$$

and solving these equations yields

$$p_c = \sqrt{\frac{\omega_c \eta_c}{\varrho_c}} \alpha(\mathcal{C}) \quad \forall c \in \mathcal{C}, \tag{18}$$

where $\mathcal{C} = \{1, \ldots, C\}$ and

$$\alpha(\mathcal{C}) = \frac{\sum_{c' \in \mathcal{C}} \sqrt{\frac{\omega_{c'} \varrho_{c'}}{\eta_{c'}}}}{B + \sum_{c' \in \mathcal{C}} \frac{\varrho_{c'}}{\eta_{c'}}}. \tag{19}$$

These prices fulfil constraint (15a). Moreover, they are also non negative (i.e., the prices satisfy the lower limits imposed by constraints (15b)). However, there can be some CF-mMIMO network operators for which $p_c > \omega_c \eta_c / \varrho_c$ or, equivalently, there can be some network operators for which $\sqrt{\omega_c \eta_c / \varrho_c} < \alpha(\mathcal{C})$. To offer an optimal solution for this potential scenario, an iterative procedure is proposed in Algorithm 1 that draws inspiration from the waterfilling

$$\text{SINR}_{ck} = \frac{p_{ck} \left| \boldsymbol{v}_{ck}^H \hat{\boldsymbol{h}}_{ck} \right|^2}{\sum_{\substack{k'=1 \\ k' \neq k}}^{K_c} p_{ck'} \left| \boldsymbol{v}_{ck}^H \hat{\boldsymbol{h}}_{ck'} \right|^2 + \boldsymbol{v}_{ck}^H \left(\sum_{k'=1}^{K_c} \boldsymbol{C}_{ck'} \right) \boldsymbol{v}_{ck} + \sigma_u^2 \left\| \boldsymbol{v}_{ck} \right\|^2}, \tag{6}$$

Algorithm 1 Solving the Stackelberg Game

Input:
B, $\mathcal{C}$, and η_c, ω_c, ϱ_c $\forall c \in \mathcal{C}$
Initialize:
$\mathcal{C}' = \mathcal{C}$, $p_c = \sqrt{\frac{\omega_c \eta_c}{\varrho_c}} \alpha(\mathcal{C})$ $\forall c \in \mathcal{C}$
while $\overline{\mathcal{C}}' = \left\{ c \in \mathcal{C}' : \sqrt{\frac{\omega_c \eta_c}{\varrho_c}} < \alpha(\mathcal{C}') \right\} \neq \emptyset$ **do**
$\check{c} = \arg\min_{c \in \overline{\mathcal{C}}'} \frac{\omega_c \eta_c}{\varrho_c}$
$p_{\check{c}} = \frac{\omega_{\check{c}} \eta_{\check{c}}}{\varrho_{\check{c}}}$ (i.e., $B_{\check{c}} = 0$)
$\mathcal{C}' \leftarrow \mathcal{C}' \backslash \check{c}$
$p_c = \sqrt{\frac{\omega_c \eta_c}{\varrho_c}} \alpha(\mathcal{C}')$ $\forall c \in \mathcal{C}'$
end while
$\boldsymbol{p}^* = \boldsymbol{p}$, $B_c^* = \frac{\omega_c}{p_c^*} - \frac{\varrho_c}{\eta_c}$ $\forall c \in \mathcal{C}$
Output:
Stackelberg point $(\boldsymbol{b}^*, \boldsymbol{p}^*)$

algorithm [46]. After initializing the set $\mathcal{C}' = \mathcal{C}$, problem **PSPR** is solved by, first, disregarding the constraint (15b) and, second, considering only the CF-mMIMO network operators in $\mathcal{C}'$ (note that the problem faced in the first iteration is the one solved in (16)-(19)). Hence, we obtain $p_c = \sqrt{\omega_c \eta_c / \varrho_c} \alpha(\mathcal{C}')$ $\forall c \in \mathcal{C}'$. If the set $\overline{\mathcal{C}}' = \left\{ c \in \mathcal{C}' : \sqrt{\omega_c \eta_c / \varrho_c} < \alpha(\mathcal{C}') \right\}$ is not empty, we select $\check{c} = \arg\min_{c \in \overline{\mathcal{C}}'} \omega_c \eta_c / \varrho_c$, set $p_{\check{c}} = \omega_{\check{c}} \eta_{\check{c}} / \varrho_{\check{c}}$ and $B_{\check{c}} = 0$ (i.e., as in the waterfilling scheme, the SP does not allocate resources to the network operator in $\mathcal{C}'$ that would otherwise decrease the revenue, thereby excluding it from the Stackelberg game), and update $\mathcal{C}' \leftarrow \mathcal{C}' \backslash \check{c}$ and check again the input condition to this loop. The procedure is iterated until all the prices satisfy constraints (15b).

Note that the operations performed by Algorithm 1 entail simple arithmetic computations within a loop with a small number of iterations (i.e., the number of cell-free operators). Additionally, the algorithm requires as input the spectral efficiencies of the cell-free networks but the computational cost associated to their estimation using (5) and (6) is negligible when compared to the cost of determining the channel estimates and combiners that cell-free networks always rely upon (see Table 5.1 in [8] for a detailed explanation of the number of operations involved in the channel estimation and combiner design steps). Overall, it can be concluded that the computational complexity of arriving at the Stackelberg solution can bee deemed as insignificant.

V. SMART CONTRACT DESIGN AND IMPLEMENTATION

In the defined system model, a SC oversees the DSS algorithm. The SP, acting as the leader in the game, publishes the available bandwidth for a specific game execution, uniquely identified by an identifier (id), within the SC. Subsequently, operators can request participation in the game by providing their parameters to the SC. At any time, the SP can request the SC to block new operators from joining this particular game. Then, the SC notifies the operators that the game, clearly identified by the id, is set to commence and subsequently resolves the game.

We explore two potential scenarios for game resolution: 1) the SP autonomously resolves the game and publishes the results in the SC, or 2) the SC autonomously resolves the game. In both scenarios, the results must be published in the SC, communicated to the participants, and remain auditable by any entity, including third parties not directly engaged in the game. Furthermore, it is assumed that neither the SP nor the operators require the setup, administration, or maintenance of a blockchain network.

Next, the most suitable blockchain for the considered scenario is identified, and the operational logic of the smart contract responsible for managing the DSS algorithm is defined.

A. SELECTING THE BLOCKCHAIN PLATFORM

The blockchain is a distributed and immutable database in which blocks (containing transactions) are added in such a way that two consecutive blocks are chained, making it difficult or impossible to alter the content of the database. Every transaction is signed by the entity initiating the publication request, ensuring that it cannot be rejected later. This feature will enable the SP and the CF-mMIMO network operators to record both the input parameters and the outcomes of the Stackelberg game on the blockchain.

Blockchains fall into two main categories: public and private. Public blockchains, open to all, provide a decentralized and trustless environment, with security strengthening as the number of nodes increases. Conversely, private blockchains, controlled by an authority, have limited authorized nodes, making them generally weaker against Byzantine attacks[1] due to factors like centralization and limited node diversity. While public blockchains are more resistant to Byzantine attacks, private blockchains offer privacy and control, making them suitable for specific enterprise applications, albeit with compromises in security. In this work we advocate for using a public blockchain in the Stackelberg game process to ensure transparency and security, avoiding the need for trusted entities or maintaining a private infrastructure.

Some public blockchains provide a solution to execute SCs. A SC is a piece of code that is hosted in the blockchain nodes, and the owner (or the authorized entities) can enforce its execution (with the necessary input parameters) when deemed appropriate. Ethereum was the first public blockchain introducing the possibility to deploy SCs developed in Solidity language, which could then be executed in a Turing-complete virtual machine, the so-called Ethereum virtual machine (EVM) [48]. This feature has been included in other public blockchains that are also based on EVM, such as Binance Smart Chain (BSC) or Polygon. Given the widespread acceptance and use of EVMs, we have

[1] A Byzantine attack occurs when a subset of nodes within a decentralized network behaves maliciously, undermining network consensus and reliability, potentially resulting in issues like incorrect transaction confirmations and double-spending [47].

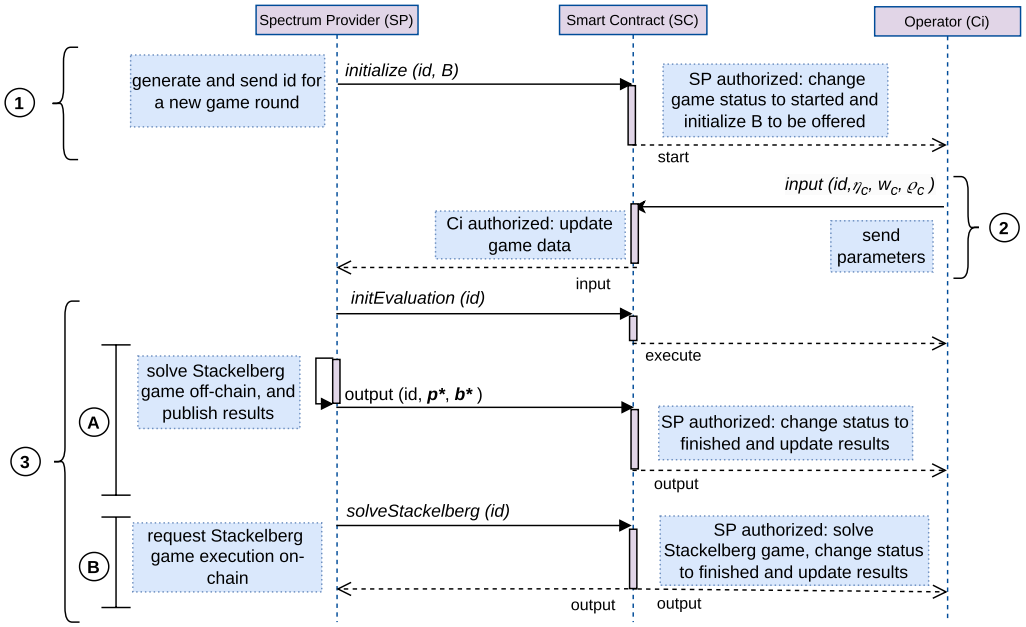

FIGURE 2. DSS protocol comprising the Stackelberg game solution and blockchain-related operations.

chosen to employ one for enabling a SC to oversee the entire Stackelberg game process, starting from the initial allocation of bandwidth by the SP to the final determination of the game results.

B. SMART CONTRACT LOGIC

In the proposed scenario (see Fig. 1), all participants (the SP and the network operators) need a blockchain account (or blockchain address) to participate in the spectrum trade. The SP must know these addresses to allow operators to publish their network parameters on the blockchain. Then, the SP deploys the SC to manage the DSS protocol with a list of the network operators' addresses and the offered bandwidth as input parameters. Even though the SP provides an initial list of network operators, this can be updated at any time thereafter. Similarly to the network operators list, the SP has the ability to modify the offered bandwidth for each round of the game. The SP must share the address of the deployed SC with the operators. This step is essential to facilitate the communication of SC updates to operators. For instance, it facilitates the delivery of notifications to operators regarding the commencement of a new round in the Stackelberg game. The SC uses a mechanism labeled as event[2] to deliver notifications to participants in the game. It serves as a communication channel through which the SC can interact with the game participants, enabling real-time updates and coordination within the Stackelberg game. The SC emits an event at each step of the DSS algorithm. For example, an event is generated when the SP specifies the available bandwidth for a particular game, or when a network operator submits their parameters for a specific round of the game. This systematic use of events ensures that all participants in the game remain informed of the relevant information throughout the process.

Following the deployment of the SC, the execution of the Stackelberg game model can start. In summary, the proposed DSS protocol consists of the following steps (see Fig. 2):

(1) The SP calls the initialize function of the SC to generate and publish a unique identifier (id) associated to this Stackelberg game round, along with the available bandwidth for that game round. The SC checks whether the SP is authorized to create a new round of the Stackelberg game, and emits an event to communicate both the offered bandwidth and the identifier of this new round to the network operators. The SP has the flexibility to establish an optional time frame for the completion of step 2. At this point, the game is considered to have started.

(2) Each CF-mMIMO operator publishes its parameters (i.e., w_c, η_c and ϱ_c) on the blockchain at every game round (identified by *id*) and executes the *input* function of the SC that, after checking whether the calling operator is authorized (i.e., whether its blockchain address is found in the list of authorized addresses provided by the SP), emits an event to communicate to the SP the parameters w_c, η_c and ϱ_c provided by the calling operator.

(3) The SP calls the *initEvaluation* function to signal the start of the Stackelberg game round. At this point, two different approaches are considered to solve the Stackelberg game:

   (a) *Off-chain approach*: The SP solves the Stackelberg game off-chain and calls the *output* function of the SC to publish the results of the game, that

[2] An event is a mechanism used in blockchain smart contracts to notify external entities or participants about specific occurrences or changes within the smart contract's state [49].

is, the resulting optimal vectors $\boldsymbol{b}^*$ and $\boldsymbol{p}^*$. The SC checks whether the SP is authorized to publish these data, and emits an event to communicate the outcome to the operators. Despite the fact that the SP conducted the execution of the game locally, all participants possess knowledge of the algorithm and input parameters, enabling them to validate the accuracy of the game-solving output.

(b) *On-chain approach*: The SP requests the SC to solve this game round. The SC checks whether the SP is authorized to publish data, and solves the Stackelberg game on-chain. Once the results are obtained, the SC stores them on the blockchain and emits an event to communicate the outcome to both the SP and the CF-mMIMO network operators. In this scenario, the Stackelberg algorithm is implemented within the SC, allowing all participants to audit the execution of the game-solving process.

Every SC function call is digitally signed by the entity originating the call and recorded on the blockchain. This not only ensures the integrity and authenticity of the provided data but also provides evidence of all the steps undertaken throughout the entire game process. That is, the information about who initiated the call to the SC, when it was made, and the specific data provided are recorded and publicly available.

Note that steps (1) and (2) rely on the assumption that the SP and each CF-mMIMO network operator commit to accept the result of the execution of the Stackelberg game. Therefore, once step (2) is completed, the contract is considered as signed, and the results published in steps (3)(a) and (3)(b) bind all the actors involved in steps (1) and (2). If any of the participants has provided incorrect data, the dishonest actor can be held responsible since the transactions of steps (1) and (2) have been signed by all parties. In conclusion, the protocol meets the fairness requirement.

VI. NUMERICAL RESULTS

A. STACKELBERG EQUILIBRIA IN CELL-FREE NETWORKS

We start by first studying how the different characteristics of the cell-free networks relate to the Stackelberg game equilibrium and how these influence, on the one hand, the resulting price and bandwidth allocations and, on the other hand, the utility perceived by the CF-mMIMO network operators. Unless otherwise stated, a default simulation setup is considered where the coverage area under analysis consists of a square of side $D = 1000$ meters over which the APs and MSs of the different CF-mMIMO networks are independently and randomly (uniformly) distributed. In order to avoid boundary effects, the nominal squared coverage area is wrapped-around by eight identical neighbor replicas. A TDD frame size equal to $\tau_{f_c} = 200$ samples is considered, and the default size of the UL training phase is set to $\tau_{p_c} = 20$ samples. Even though we are only analyzing the achievable spectral efficiency in the UL, we assume without loss of essential generality that almost the same number of frequency-time resources are allocated to both UL and DL payload data transmission phases and thus, $\tau_{uc} = \lfloor(\tau_{f_c} - \tau_{p_c})/2\rfloor$. The bandwidth available at the SP is set to $B = 40$ MHz, the power available at the MSs is set to $P_u = P_p = 100$ mW, where P_u is the maximum power available at the MSs, and the UL receiver noise powers are set to $\sigma_u^2 = -94.93$ dBm. A centralized UL operation based on the use of MMSE combiners is assumed (see [8, Corollary 5.3]) where the fractional power control algorithm proposed by Demir et al. in [8, eqn. (7.34)] is implemented with $\upsilon = -1/2$. The large-scale channel propagation gains between APs and MSs has been modelled as in [8, Sect. 2.5.2]. Moreover, assuming that the APs are equipped with half-wavelength-spaced uniform linear arrays (ULAs), the spatial correlation matrices $\boldsymbol{R}_{cmk}$ have been computed using the local scattering model described in [8, Sect. 2.5.3, eq. (2.18)] and setting both the azimuth and elevation angular standard deviations (ASDs) to $\sigma_\varphi = \sigma_\vartheta = 15^o$. This model has been shown appropriate to characterize ULAs, expected to be found in the small-sized APs conforming cell-free networks. All the numerical results shown next correspond to the outcomes of 10000 random scenarios with their corresponding Stackelberg solutions and, unless otherwise stated, the network weighting and normalizing coefficients have been set to $\omega_c = 1$ currency units and $\varrho_c = 10^7$ bit/s, respectively, for all $c \in \mathcal{C}$.

TABLE 2. Impact of the number of network operators on the results of the Stackelberg game.

C	$\overline{B}_c$ (MHz)	$\overline{p}_c$ (CU/MHz)	$\overline{U}_c$ (CU)	$\overline{R}_{\text{SP}}$ (CU)
2	20	0.050	4.768	1.994
5	8	0.124	3.861	4.961
10	4	0.246	3.183	9.845

Solving the Stackelberg game is only required, at most, whenever there are significant changes in the large-scale propagation conditions (i.e., the number of active APs, the number of active MSs, or the achievable spectral efficiencies) that usually occur on a time scale of tens or even hundreds of coherence blocks. Consequently, and owing to its low computational complexity, the game execution time can be well accommodated within this interval. As done in most of the literature, the simulation results shown next correspond to a specific network configuration using many distinct static scenarios (each with fixed large-scale parameters) and they serve as indicative outcomes that would be observed over different periods of time in a dynamic scenario. The simulation framework just described has been implemented in Matlab and executed on a personal computer equipped with an Intel Core i7 with 32 GB of RAM.

1) IMPACT OF THE NUMBER OF NETWORK OPERATORS

In order to gain a first insight into the operation of the Stackelberg game, results have been generated by considering different numbers of cell-free operators under the assumption

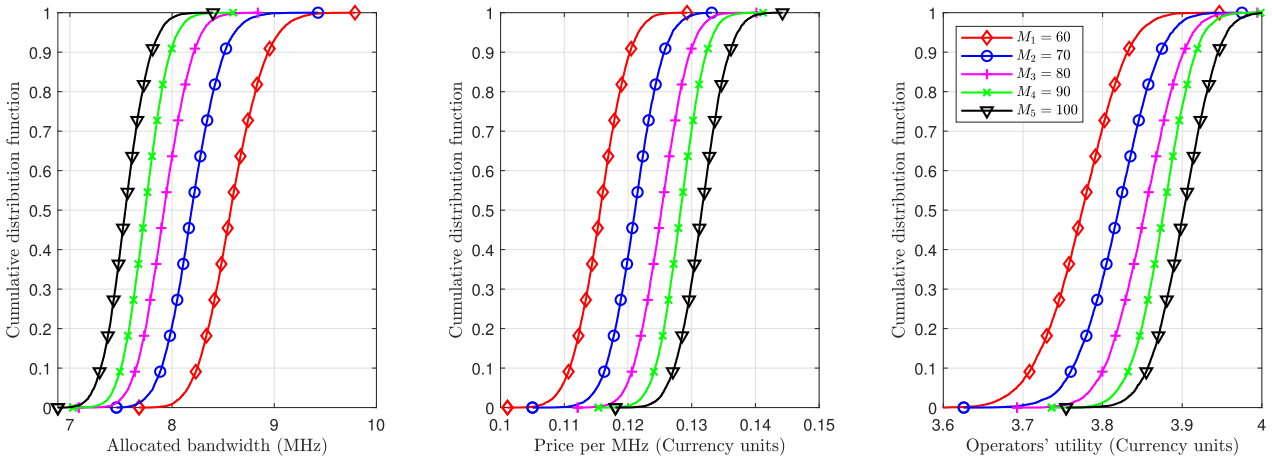

FIGURE 3. Impact of the number of APs in the network on the allocated bandwidth (left), price per MHz (middle) and operators' utility (right).

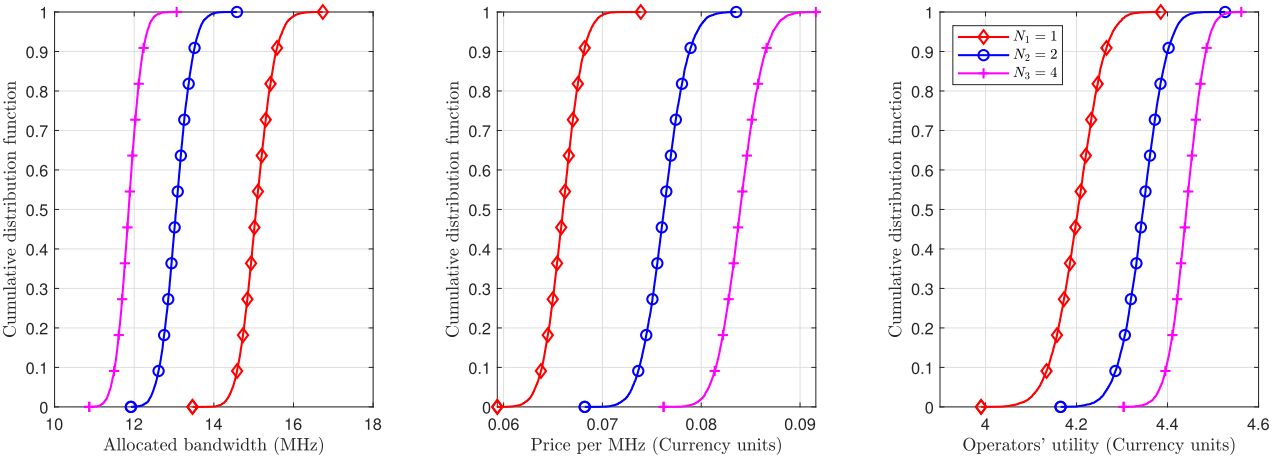

FIGURE 4. Impact of the number of antennas per AP on the allocated bandwidth (left), price per MHz (middle) and operators' utility (right).

that all networks have the same parameters and serve the same number of MSs. In particular, a setup has been considered in which every CF-mMIMO network consists of $M_c = 80$ APs, each equipped with $N_c = 2$ antenna arrays, and serving $K_c = 30$ MSs. Note that since all CF-mMIMO networks have the same parameters, their average SEs will be identical. As a result, an even split of the frequency resources is to be expected among the players. Table 2 presents the Stackelberg game results when considering that there are $C = 2$, 5, or 10 network operators competing for the available bandwidth. This table provides the average assigned bandwidth to each operator ($\bar{B}_c$), the average price paid per MHz ($\bar{p}_c$), the average operators' utility ($\bar{U}_c$) and the average revenue of the SP ($\bar{R}_{\text{SP}}$). In agreement with intuition, as the number of operators participating in the game increases, each of them receives, on average, a proportionally smaller fraction of the available bandwidth. Having more operators on the game leads to an increase in the price per MHz each of them has to pay to get the bandwidth assigned. Interestingly, the utility that the acquired bandwidth brings to each operator diminishes as C increases. This is an indication that small chunks of bandwidth bring little value to the operator. Note that this trend could help to naturally limit the number of operators actually interested in joining the game as a point will be reached where an operator will render the expected utility to be gained as insignificant. Exactly the opposite behaviour is observed on the revenue obtained by the SP: the more operators wishing to join the game, the higher the average revenue obtained. The overall conclusion from these results matches the intuition underlying any competition for a scarce resource: the owner of the resource strives to attract a large number of consumers, which leads to soaring prices and revenues, while the consumers are willing to pay higher prices in a context of increased competition up to a point when the resource becomes too expensive, and their utility plummets.

2) IMPACT OF THE NETWORK DENSIFICATION

For the first set of results, a configuration with $C = 5$ CF-mMIMO networks is considered, each with a different number of APs ($M_1 = 60$ APs, $M_2 = 70$ APs, $M_3 = 80$ APs, $M_4 = 90$ APs, $M_5 = 100$ APs) intended to highlight

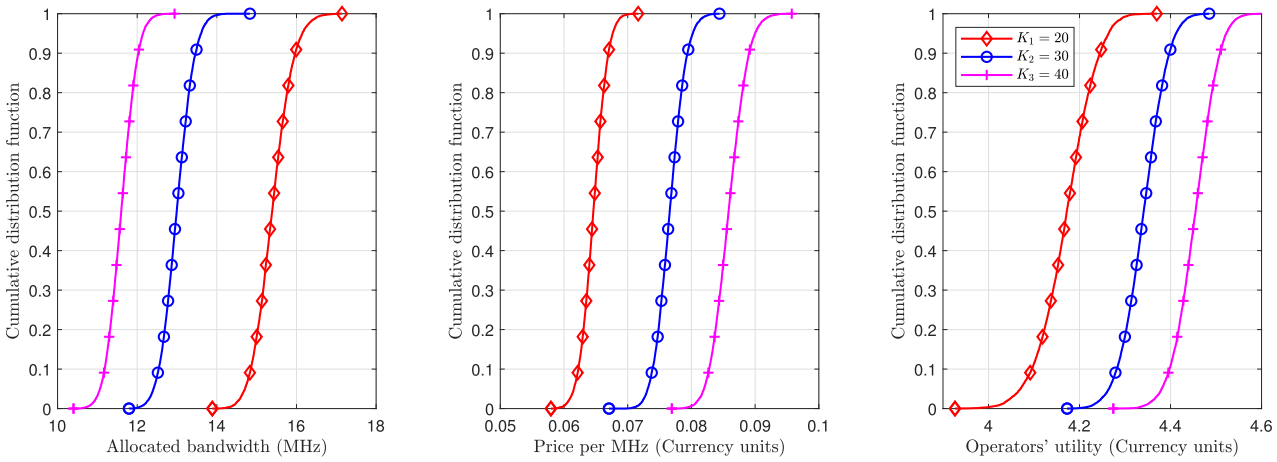

FIGURE 5. Impact of the network load on the allocated bandwidth (left), price per MHz (middle) and operators' utility (right).

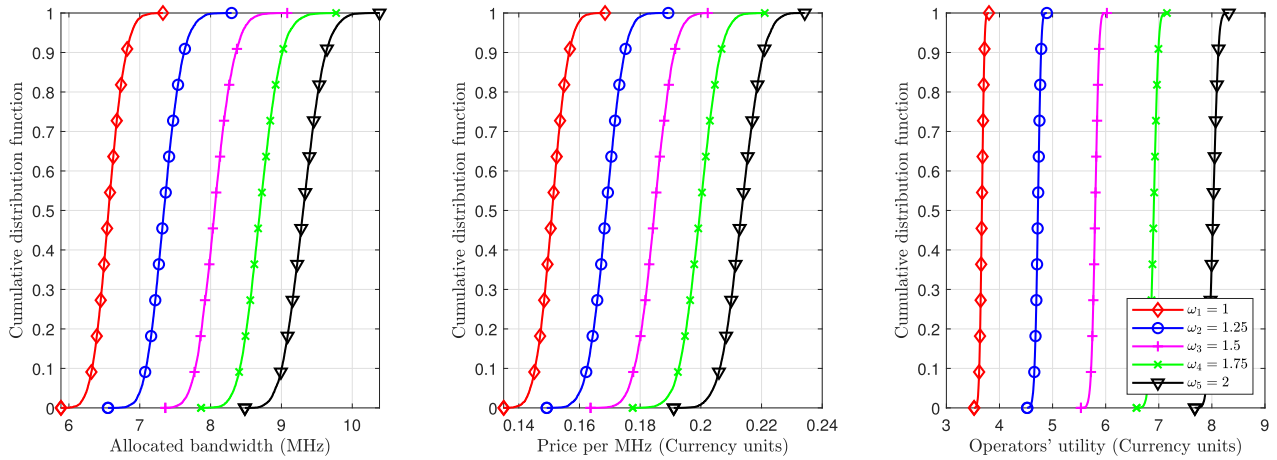

FIGURE 6. Impact of the network weighting coefficients on the allocated bandwidth (left), price per MHz (middle) and operators' utility (right).

how the differences in spectral efficiency among the CF-mMIMO segments caused by varying degrees of network densification affect the Stackelberg game solutions. In this scenario, $K_c = 30$ MSs are assumed active for all $c \in \mathcal{C}$ and each AP in the system has been assumed to be equipped with $N_c = 2$ antennas.

Fig. 3 depicts the cumulative distribution functions (CDFs) of the allocated bandwidth (left), price to be paid per MHz (middle), and utility perceived by the network operators (right). Focusing first on the allocated bandwidths, it is clearly observed that the more APs a network has, the less bandwidth it gets allocated and the higher the price it pays for it. It may seem counterintuitive that the network with the highest physical layer achievable spectral efficiency is penalized by being assigned less bandwidth while paying the highest price per MHz. Recall, however, that the Stackelberg solution aims to maximize both the SP revenue and the network operators' utility. Indeed, the operators' utility (see Fig. 3-right) can be seen to increase in accordance with the level of network densification. In other words, having a densely deployed network allows the operator to provide services using less bandwidth, and despite the higher investment required to pay for the assigned bandwidth, it is expected that the operator will be able to commercialize it in a more profitable manner among its subscribers. It is worth pointing out that the operators' utility, although increasing with network densification, seems to obey a law of diminishing returns, whereby successive increases in the number of APs bring progressively smaller benefits.

3) IMPACT OF THE NUMBER OF ANTENNAS AT THE APs

The numerical results presented in Fig. 4 are the outcome of a similar analysis to that performed when evaluating the impact of the network densification. In this case, however, we consider a setup where $C = 3$ CF-mMIMO network operators have $M_c = 80$ APs, each equipped with $N_1 = 1$, $N_2 = 2$, or $N_3 = 4$ antennas per AP, respectively. Each of these operators is serving a total of $K_c = 30$ MSs, and they are competing for the available bandwidth provided by the SP. A very similar trend to that observed in the case

of varying the number of APs can be noticed when varying the number of antennas per AP. In particular, enhancing the network's spectral efficiency by increasing the number of antennas at each AP invariably leads to a smaller portion of bandwidth being assigned, and moreover, it has to be acquired at a higher price per MHz, as seen in Figs. 4-left and -middle. Nonetheless, the operators' utility, governed by the maximization of (9), increases with the number of antennas (Fig. 4-right), on the expectation that the operator will be able to better monetize the assigned bandwidth thanks to its superior performance metrics. Again, note that increases in operators' utility will likely become marginal beyond a certain number of antennas per AP.

4) IMPACT OF THE NETWORK LOAD

Focus is now laid on the effect the network load has on the solution of the Stackelberg game. Numerical results presented in Fig. 5 correspond to the outcome of a setup where $C = 3$ CF-mMIMO network operators serving $K_1 = 20$, $K_2 = 30$, and $K_3 = 40$ MSs, respectively, compete to maximize their utility function under identical network characteristics ($M_c = 80$ APs, $N_c = 2$ antennas per AP). Fig. 5-left clearly indicates that the more loaded a network is, the less bandwidth it gets assigned. Note that increasing the number of MSs a network is serving, while guaranteeing that $M_c N_c \gg K_c$, leads to an increase in the aggregate spectral efficiency of the network and, thus, in line with previous outcomes, results in less bandwidth being assigned and also in a higher expenditure to purchase it (see Fig. 5-middle). Interestingly, however, the operators' utility, shown in Fig. 5-right, increases with the network load clearly suggesting that the corresponding operator would eventually be able to obtain more economic value by serving a larger number of MSs.

5) IMPACT OF THE NETWORK WEIGHTING COEFFICIENTS

Concluding this exploration on the interrelation between the CF-mMIMO topology and the Stackelberg solution to the problem of bandwidth allocation, we consider in this subsection the case where, for some reason related to the resource allocation process, the different network operators agree to use different weighting coefficients. Towards this end, a setup is considered where $C = 5$ CF-mMIMO networks with $M_c = 80$ APs, each equipped with $N_c = 2$ antennas and providing service to $K_c = 30$ MSs, are assigned network coefficients $\omega_1 = 1$, $\omega_2 = 1.25$, $\omega_3 = 1.5$, $\omega_4 = 1.75$, and $\omega_5 = 2$ (measured in currency units). Results shown in Fig. 6 reveal the effect of this prioritization mechanism: the larger the weighting coefficient, the more bandwidth the corresponding network is assigned (Fig. 6-left) and the higher the price becomes (Fig. 6-middle). Correspondingly, the operators' utility also increases with the assigned weight (Fig. 6-right). Note that, in light of these results, the weighting coefficients can be used to provide different priority levels to the network operators competing to access the bandwidth sold by the SP. In particular, the weighting coefficients could be used as an equalizing mechanism if the SP wishes to equally distribute the available bandwidth among networks with dissimilar spectral efficiencies due to, for instance, varying degrees of densification or different network loads.

B. BLOCKCHAIN PERFORMANCE ASSESSMENT

In this section, the suitability to use an EVM-based public blockchain in the proposed DSS protocol is analyzed. As previously stated, the use of public blockchains comes at a cost: each time either a network operator or the SP interact with the SC deployed on the blockchain, there are fees to be paid, which depend on various issues such as the complexity of operations to be performed and the speed at which transactions need to be published. Critically, the higher the complexity of the functions and/or the shorter the delay required, the more expensive the blockchain-related processing becomes. Consequently, it is worth analyzing the cost associated to the execution of the Stackelberg game functions and the trade-off between cost and delay.

1) GAS COST OF THE STACKELBERG GAME FUNCTIONS

As explained in section V, a SC has been implemented that can be deployed and executed on any EVM-based blockchain. The SC has been implemented using the Solidity language [49], and it has been deployed using the Hardhat Network, a local Ethereum network node designed for development [50]. This approach enables deploying, testing and debugging the code of the SC, all in a local environment and without a real cost. The proposed SC defines five functions corresponding to the ones specified in the design of the system:

- *initialize*: the SP executes this function to allow operators calling the *input* function.
- *input*: each operator aiming at participating in this spectrum assignment round executes this function to make its parameters (i.e., w_c, η_c and ϱ_c) available.
- *initEvaluation*: the SP executes this function to signal that the Stackelberg game starts.
- *output*: the SP executes this function to publish the outcome (price and bandwidth per CF-mMIMO operator) of the Stackelberg game (computed off-chain) for this spectrum assignment round.
- *solveStackelberg*: the SP executes this function to compute the Stackelberg game on-chain and publishes the results (price and bandwidth per CF-mMIMO operator).

In an EVM-based blockchain, the cost to execute any transaction is independent on the environment in which the SC is executed, it is measured in gas units and specified in the Ethereum Yellow Paper [48]. Several utilities facilitate the task of obtaining the costs, in gas units, of executing each function. The hardhat-gas-reporter plugin[3] has been used in

[3]Gas metrics for method calls and deployments on L1 and L2 blockchain networks. Available: https://www.npmjs.com/package/hardhat-gas-reporter, accessed on 1 April 2024.

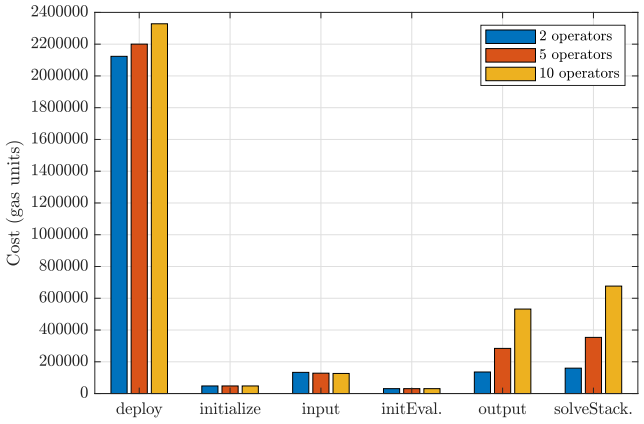

FIGURE 7. Cost, measured in gas units, associated to the execution of the Stackelberg game functions.

this work as it enables a simple generation of gas consumption reports for each function.

Fig. 7 displays the costs (measured in gas units) of the five functions comprising the proposed solution, as well as the cost to deploy the SC. Note that the cost to deploy the SC in the blockchain network is higher compared to the cost associated with the execution of other functions. However, it is important to observe that the SC is deployed only once and used multiple times for different rounds of the Stackelberg game.

As the *initialize* and *initEvaluation* functions are only executed once per spectrum assignment round, and the input parameters are constant in size, the corresponding costs remain fixed regardless of the number of CF-mMIMO network operators participating in the game.

At every spectrum assignment round, the *input* function is executed once by each operator. The operators provide parameters that must be recorded on the SC memory, which is an expensive operation. According to Appendix G of the Ethereum Yellow Paper [48], the gas cost of adding a new element to an array is 20000 gas units and the gas cost of adding a successive element to this array is 5000 gas units (2100 for accessing and 2900 for modifying it), which results in a difference of 15000 gas units. Consequently, the first time the function is executed, the gas cost is higher than that in successive executions and the average cost of the *input* function (cost per operator) decreases slightly as more network operators take part in the game. As it will be shown in Section VI-B2, this extra cost can be considered negligible when compared to the total price of executing the function.

The cost of the *output* function, corresponding to solving the game off-chain, increases linearly with the number of network operators participating in the Stackelberg game. This is to be expected since the same operations must be performed by each operator participating in the game.

Compared to the cost associated with the off-chain execution of the *output* function, the on-chain execution of the *solveStackelberg* function brings along an increase of 24% and 27% for the $C = 5$ and $C = 10$ network operators scenarios, respectively. The cost increments associated to the *solveStackelberg* function stem from the action of storing the resulting bandwidths and prices in memory.

2) TRADE-OFF BETWEEN COST AND DELAY

The cost, measured in gas units, provides useful information about the complexity of the operations, as well as a means to compare different solutions because this metric is not affected by the price fluctuations of the associated cryptocurrency. However, the economic cost of running the different tasks involved in a Stackelberg game round can change daily as a result of the fluctuations of the price of the associated cryptocurrency. Therefore, the final price of executing a function is calculated as the gas units needed to run a function (see Fig. 7) multiplied by the gas price. The gas price refers to the amount of Wei[4] that a user is willing to pay for every unit of gas. In addition, the gas price at a given time may differ considerably from one blockchain to another.

Public blockchains can be classified into Layer 1 and Layer 2 based on their architecture (see Table 6). In the context of EVM-based blockchains, Ethereum is recognized as a leading Layer 1 blockchain and the second-largest cryptocurrency by market share according to CoinMarketCap,[5] offering a robust and well-established environment for SC execution, making it a preferred solution. On the other hand, Polygon is a widely used Layer 2 blockchain with the highest number of deployed SCs, and designed to enhance Ethereum's scalability, thus translating into cost reduction for the execution of SCs. Thus, to evaluate the cost of using public blockchains for our proposed system, we first conduct a detailed analysis of the cost of our solution on both Ethereum and Polygon, and then we summarize the cost analysis of all selected blockchains in Table 6.

Figs. 8a and 8b illustrate the average costs, over a 12-month period (July 2022 to July 2023), associated to the deployment of the SC and the execution of its functions when using Ethereum and Polygon, respectively. The costs in Ethereum can get really high. For example, the cost of executing the SC can reach up to $700. In contrast, the average costs of executing the functions of the SC are much lower. For example an operator could pay about $7 for publishing its network parameters, and the SP could pay about $14 for publishing the game results. Let us assume that a round of the Stackelberg game is executed once every 15 min, this means that 96 rounds of the game should be executed per day. This could entail a daily cost of about $1,344 on average just for the SP to publish the game results, and $672 for each operator on a daily basis. Additionally, the *initialize* and the *initEvaluation* functions bring along an additional average

[4]Wei refers to the smallest denomination of Ether (ETH), the currency used on the Ethereum network (1 ETH = 10^{18} Wei). This unit is also used by other EVM-based blockchains.

[5]CoinMarketCap: Cryptocurrency Market Capitalizations. Source: https://coinmarketcap.com/. Data publication date: 1 April 2024.

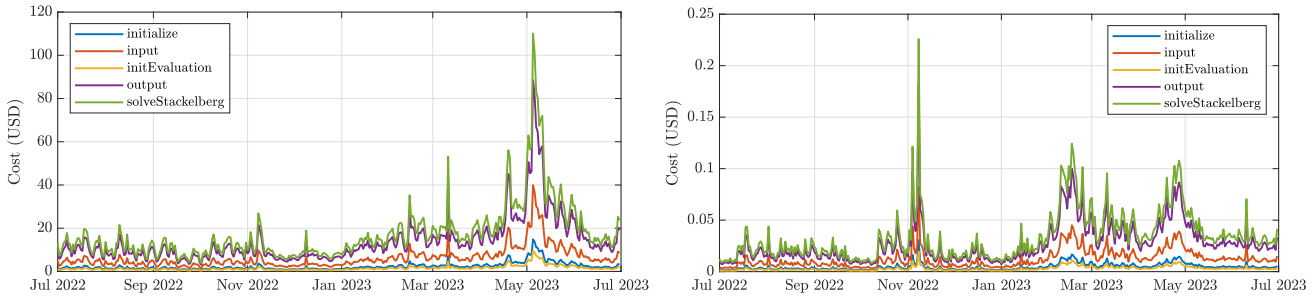

(a) Ethereum (b) Polygon

FIGURE 8. Estimated average cost of the main functions (measured in USD) over a 12-month period (July 2022 to July 2023) considering the average gas price.

TABLE 3. Summary of the estimated cost of the proposed solution (in US dollars) for $C = 5$ CF-mMIMO networks and considering the average, maximum and minimum gas prices paid over a 12-month period (July 2022 to July 2023).

		deployment	*initialize*	*input*	*initEval.*	*output*	*solveStack.*
Ethereum	avg.	106.929	2.325	6.234	1.497	13.81	17.186
	max.	684.545	14.884	39.909	9.585	88.458	110.025
	min.	23.829	0.518	1.389	0.333	3.079	3.830
Polygon	avg.	0.421	0.009	0.025	0.006	0.054	0.067
	max.	2.810	0.061	0.164	0.039	0.363	0.452
	min.	0.101	0.002	0.006	0.001	0.013	0.016

cost of \$3.82 per game round, which results in a daily cost of \$367 for the SP.

When Polygon is used, the costs are significantly reduced. As shown in Fig. 8b and Table 3, the costs do not exceed \$3 for deploying the contract (\$0.42 on average), \$0.17 for publishing the parameters of the network operators (\$0.02 on average) and \$0.37 for publishing the results (\$0.05 on average). In this case, the cost of performing a game round once every 15 minutes entails, on average, a total cost of \$5.2 to the SP to publish the game results and \$2.4 per operator and day. Additionally, the *initialize* and the *initEvaluation* functions bring along an additional average cost of \$0.015 per round, which totals a daily cost of \$1.44 for the SP.

The economic viability of the proposed solution has been analyzed based on the average price to execute a function on the blockchain. However, the delay introduced by the use of the blockchain is also an important factor that may affect the final costs. In general, and given a particular blockchain, whenever a function has to be executed within a shorter time span, a higher price needs to be paid as a fee. A game round involves sequentially executing the functions *initialize*, *input*, *initEvaluation*, and *output*. Therefore, the total delay can be obtained as the sum of the delays incurred by each function. Here, we consider the best-case scenario, where all *input* functions (one per network operator) are published in the same block. If, instead, each *input* function is published in a different block, the delay associated with the *input* function corresponding to the last operator publishing its parameters is the one that must be considered. Note, however, that the SP decides when the game must be solved. Thus, the SP can establish a maximum waiting time for the publication of all operators' parameters.

TABLE 4. Trade-off between delay and price for $C = 5$ CF-mMIMO networks; average price for a minimum delay in Ethereum and Polygon.

	Ethereum	Polygon
delay	45-110s	5-10s
price		
initialize	\$7.486	\$0.007
input	\$22.214	\$0.022
initEval.	\$4.821	\$0.028
output	\$44.491	\$0.044
solveStack.	\$55.338	\$0.052

Table 4 illustrates a trade-off between delay and price considering $C = 5$ CF-mMIMO network operators when aiming at a minimum delay for both Ethereum and Polygon. In Ethereum, a custom script based on [51] was executed to fetch the estimated transaction delays associated with gas prices ranging from 1 Gwei to 100 Gwei over a year period (July 2022 to July 2023). The minimum delays are obtained for a gas price of 100 Gwei, which is the highest gas price that is considered. The evaluation of all delays associated to this gas price resulted in an average delay per operation of around 2 minutes. Given this average delay per operation, the total delay of a Stackelberg game round is around 8 minutes in the best scenario. In this case, an operator could pay

approximately \$22 for publishing its network parameters, while the SP would be required to make a payment of approximately \$44 for publishing the game outcomes. The average price for executing the game on-chain reaches up to \$55.

In Polygon, we did not find any similar data source to extract the estimated delay of a blockchain transaction given the gas price. To perform the evaluation, the minimum delay provided by Polygonscan [52] was considered, which ranges between 5 and 10 seconds. Taking into account this range, the delay associated with the execution of a Stackelberg game round can vary from 20 to 40 seconds. Using a custom script to fetch the gas price corresponding to this specific delay range throughout the time span of June and July 2023, the estimated costs were approximately one thousand times cheaper than those in Ethereum: about \$0.022 for publishing network parameters, \$0.044 for publishing the game results, and \$0.052 for executing the game on-chain. Thus, it can be concluded that employing Polygon results in significantly lower delays and substantially reduced economic costs compared to those incurred when using Ethereum.

Table 5 summarizes the estimated costs (using Polygon) to be paid by the SP and by each operator, on a daily and monthly basis, to periodically participate in the game. In particular, three different rates are considered: every minimum theoretical block time (10 seconds for Polygon), every 10 minutes and every hour. As expected, increasing the frequency of execution in Stackelberg game rounds results in an increase in costs. However, as the spectral efficiency provided by the CF-mMIMO network operators may vary over time, the more frequent execution allows for a better adaptability of the spectrum usage to the changes experienced by the network conditions. A thorough analysis of this trade-off constitutes an interesting avenue for further research.

To conclude, Table 6 provides a comparative summary of the average economic cost associated with executing a round of the Stackelberg game, both on-chain and off-chain. As observed, Ethereum incurs the highest cost, exceeding \$50, followed by BSC at approximately \$2. Optimism emerges as the network with the lowest economic cost, followed by Fantom, Polygon, and Arbitrum. Anyway, note that the difference between the most cost-efficient blockchains is relatively small; for instance, the cost difference between Polygon and Optimism is just 16 cents

3) BLOCKCHAIN PERFORMANCE MEASURED IN TRANSACTIONS PER SECOND

In addition to the economic costs and transaction publication delays on the blockchain, the performance and scalability of the blockchain network has been analyzed. For this purpose, the number of transactions per second (TPS) that can be achieved across six blockchains has been examined, including three Layer-1 and three Layer-2 blockchains operating with Ethereum as Layer-1 (see Table 6).

TABLE 5. Estimated cost summary for executing a complete Stackelberg game round per day and per month, considering various frequencies and utilizing Polygon.

		Polygon		
		10s	10min	1h
daily cost	SP	\$596.16	\$9.94	\$1.66
	operator	\$216	\$3.60	\$0.60
monthly cost	SP	\$17,884.80	\$298.08	\$49.68
	operator	\$6,480	\$108	\$18

The maximum theoretical throughput is defined as the number of transactions that can be included in a block divided by the block duration. The block capacity, measured in gas units, determines the maximum number of transactions a block can hold. Table 6 shows that almost all the considered blockchains allow up to 30 million gas units per block, except BNB, which allows up to 140 million. Additionally, the block duration is set by design for each blockchain. For example, Arbitrum has the shortest theoretical block duration set to 0.25 seconds, while the block duration of Ethereum, set to 12 seconds, is the longest one. With this data, the maximum throughput that the blockchain network can support can be evaluated. For instance, Arbitrum, with a block duration of nearly 0.25 seconds and a block gas limit of 32 million, could theoretically accommodate about 1,428 transactions in a single block, resulting in a maximum theoretical throughput of 6,095 TPS. On the other hand, Ethereum currently supports about 119 TPS, though Ethereum 2.0 aims to reach up to 100,000 TPS in the future. These performance values are theoretical, and actual performance may vary due to fluctuations in block sizes and other practical factors that affect blockchain operations. When analyzing the maximum number of transactions per second recorded on each blockchain, BNB has reached the highest throughput at 1,700 TPS, followed by Arbitrum at 532 TPS and Polygon at 180 TPS. Table 6 reports the real-time throughput over a 30-day period. As seen, Polygon achieves around 50 TPS, whereas Ethereum just attains 15 TPS. Hence, it can be asserted that blockchains have the capacity to accommodate greater loads than the ones currently supported.

Furthermore, another factor to consider when using a blockchain is the publication frequency required for each scenario. In the case of public blockchains, global network usage must be taken into account as transactions for various purposes will be published simultaneously by unknown users and applications. However, even if a network supports a high throughput, it must also provide adequate security. As explained in Section V-A, it is essential for a blockchain to be robust against attacks such as the Byzantine attack, which are less likely as the number of nodes in the blockchain network increases. Considering this, Ethereum can be regarded as the most secure blockchain (with

TABLE 6. Summary of the analysis of different EVM-based public blockchains: blockchain parameters, economic cost of our solution running on each blockchain, and blockchain performance (Data source: Chainspect, blockchain analytics platform focused on technical metrics https://chainspect.app/dashboard (Data obtained on April 17, 2024)).

	Ethereum	BSC/BNB	Fantom	Polygon	Optimism	Arbitrum
Blockchain type	Layer-1	Layer-1	Layer-1	Layer-2	Layer-2	Layer-2
Number of validators nodes	7,500	40	58	100	1	13
Number of deployed SCs (millions)	63	312	162	341	128	4
Avg. off-chain cost (USD)	50.008	1.973	0.155	0.197	0.031	0.257
Avg. on-chain cost (USD)	53.485	2.110	0.106	0.211	0.033	0.275
Block gas limit (millions)	30	140	31	30	30	32
Block time (seconds)	12	3	1	2	2	0.25
Real-Time throughput (30-day period) (TPS)	15	50	3	50	8	18
Max recorded throughput (TPS)	60	1,730	180	280	33	532
Max theoretical throughput (TPS)	119	2,000	1,470	649	714	6,095

7, 500 nodes) followed by Polygon (with 100 nodes). Other factors can also impact the security of the solution, such as the use of relatively new blockchains, which typically undergo less testing compared to more established networks like Ethereum. For instance, Polygon boasts the highest number of deployed contracts, around 341 million, whereas Arbitrum has the lowest number, approximately 4 million. Therefore, when selecting the most suitable blockchain, it is crucial to consider various requirements that can influence the viability of the system, including acceptable economic costs, publication delay and frequency, and the level of security provided.

VII. CONCLUSION

This work has presented a new DSS strategy in the context of an environment where multiple mobile operators are active. It has been further assumed that a SP is available who is interested in monetizing the spectrum it owns by selling it, as a whole or in part, to the mobile operators. Towards this end, a framework has been proposed to govern this spectrum trade that takes the form of a Stackelberg game whose solution (i.e., Nash equilibrium) strikes a compromise between the revenue the SP can obtain and the additional capacity mobile operators enjoy when acquiring extra bandwidth. An integral part of our proposal is a physical layer abstraction of CF-mMIMO networks that allows to incorporate important parameters to the Stackelberg solution while allowing an analysis of their incidence. Notably, the entire framework hinges on the robust foundation of blockchain technology, where every transaction and its accompanying data, crucial for the game's resolution, is safely recorded and secured by means of a SC. This innovative approach not only leverages the inherent advantages of blockchain, such as decentralization and immutability but also introduces a novel protocol specifically designed to safeguard the fairness, integrity, and traceability of the entire spectrum trade process. It is worth noting that the spectrum trade protocol has been assessed on two commercial blockchains, namely, Ethereum and Polygon, thus allowing to obtain realistic measurements of the overheads in terms of time and cost the use of a blockchain brings along. Numerical results have shown that improving the spectral efficiency of a given virtual operator leads to a higher price this operator has to pay to acquire the extra bandwidth building on the expectation that this network will in turn be able to charge higher fees to its customer base. Regarding the blockchain implementation, Polygon has shown to offer substantial savings in terms of delay and cost when compared to those obtained when using Ethereum.

This research has solely focused on scenarios involving a single SP within a public blockchain framework. Moving forward, our research will expand to explore more complex scenarios where multiple SPs, each owning distinct portions of the spectrum, compete to offer spectrum resources to multiple CF-mMIMO operators. This extension will enable us to investigate the dynamics of spectrum sharing and allocation in multi-provider, multi-buyer environments, considering factors such as pricing strategies, resource availability, and network performance optimization. In addition to exploring multi-provider scenarios, future work will involve evaluating alternative blockchain architectures beyond the public blockchain model. Advantages and disadvantages of using different blockchain platforms, such as private or consortium blockchains, for DSS in CF-mMIMO networks will be assessed. This analysis will provide insights into the scalability, security, and efficiency considerations associated with various blockchain technologies in facilitating spectrum trading and management.

REFERENCES

[1] C.-X. Wang, X. You, X. Gao, X. Zhu, Z. Li, C. Zhang, H. Wang, Y. Huang, Y. Chen, H. Haas, J. S. Thompson, E. G. Larsson, M. D. Renzo, W. Tong, P. Zhu, X. Shen, H. V. Poor, and L. Hanzo, "On the road to 6G: Visions, requirements, key technologies and testbeds," *IEEE Commun. Surveys Tuts.*, vol. 25, no. 2, pp. 905–974, 2nd Quart., 2023.

[2] N. Rajatheva, "White paper on broadband connectivity in 6G," 2020, *arXiv:2004.14247*.

[3] H. Tataria, M. Shafi, A. F. Molisch, M. Dohler, H. Sjöland, and F. Tufvesson, "6G wireless systems: Vision, requirements, challenges, insights, and opportunities," *Proc. IEEE*, vol. 109, no. 7, pp. 1166–1199, Jul. 2021.

[4] H. Q. Ngo, A. Ashikhmin, H. Yang, E. G. Larsson, and T. L. Marzetta, "Cell-free massive MIMO versus small cells," *IEEE Trans. Wireless Commun.*, vol. 16, no. 3, pp. 1834–1850, Mar. 2017.

[5] J. Zhang, S. Chen, Y. Lin, J. Zheng, B. Ai, and L. Hanzo, "Cell-free massive MIMO: A new next-generation paradigm," *IEEE Access*, vol. 7, pp. 99878–99888, 2019.

[6] S. Elhoushy, M. Ibrahim, and W. Hamouda, "Cell-Free massive MIMO: A survey," *IEEE Commun. Surveys Tuts.*, vol. 24, no. 1, pp. 492–523, 1st Quart., 2022.

[7] J. G. Andrews, S. Buzzi, W. Choi, S. V. Hanly, A. Lozano, A. C. K. Soong, and J. C. Zhang, "What will 5G be?" *IEEE J. Sel. Areas Commun.*, vol. 32, no. 6, pp. 1065–1082, Jun. 2014.

[8] Ö. T. Demir, E. Björnson, and L. Sanguinetti, "Foundations of user-centric cell-free massive MIMO," *Found. Trends Signal Process.*, vol. 14, nos. 3–4, pp. 162–472, 2021.

[9] M. Matinmikko-Blue, S. Yrjölä, and P. Ahokangas, "Spectrum management in the 6G era: The role of regulation and spectrum sharing," in *Proc. 2nd 6G Wireless Summit (6G SUMMIT)*, Mar. 2020, pp. 1–5.

[10] M. Giordani, M. Polese, M. Mezzavilla, S. Rangan, and M. Zorzi, "Toward 6G networks: Use cases and technologies," *IEEE Commun. Mag.*, vol. 58, no. 3, pp. 55–61, Mar. 2020.

[11] R. H. Tehrani, S. Vahid, D. Triantafyllopoulou, H. Lee, and K. Moessner, "Licensed spectrum sharing schemes for mobile operators: A survey and outlook," *IEEE Commun. Surveys Tuts.*, vol. 18, no. 4, pp. 2591–2623, 4th Quart., 2016.

[12] S. Lee, S. M. Chan-Olmsted, and H.-H. Ho, "The emergence of mobile virtual network operators (MVNOs): An examination of the business strategy in the global MVNO market," *Int. J. Media Manage.*, vol. 10, no. 1, pp. 10–21, Feb. 2008.

[13] S. Bhattarai, J. J. Park, B. Gao, K. Bian, and W. Lehr, "An overview of dynamic spectrum sharing: Ongoing initiatives, challenges, and a roadmap for future research," *IEEE Trans. Cognit. Commun. Netw.*, vol. 2, no. 2, pp. 110–128, Jun. 2016.

[14] E. A. Jorswieck, L. Badia, T. Fahldieck, E. Karipidis, and J. Luo, "Spectrum sharing improves the network efficiency for cellular operators," *IEEE Commun. Mag.*, vol. 52, no. 3, pp. 129–136, Mar. 2014.

[15] T. Irnich, J. Kronander, Y. Selén, and G. Li, "Spectrum sharing scenarios and resulting technical requirements for 5G systems," in *Proc. IEEE 24th Int. Symp. Pers., Indoor Mobile Radio Commun. (PIMRC Workshops)*, Sep. 2013, pp. 127–132.

[16] H. Kamal, M. Coupechoux, and P. Godlewski, "Inter-operator spectrum sharing for cellular networks using game theory," in *Proc. IEEE 20th Int. Symp. Pers., Indoor Mobile Radio Commun.*, Sep. 2009, pp. 425–429.

[17] Z. Ji and K. J. Liu, "Cognitive radios for dynamic spectrum access–dynamic spectrum sharing: A game theoretical overview," *IEEE Commun. Mag.*, vol. 45, no. 5, pp. 88–94, May 2007.

[18] N. Asokan, M. Schunter, and M. Waidner, "Optimistic protocols for fair exchange," in *Proc. 4th ACM Conf. Comput. Commun. Secur. (CCS)*, 1997, pp. 7–17.

[19] B. Pfitzmann, M. Schunter, and M. Waidner, "Optimal efficiency of optimistic contract signing," in *Proc. 17th Annu. ACM Symp. Princ. Distrib. Comput. (PODC)*, 1998, pp. 113–122.

[20] J. A. Garay, M. Jakobsson, and P. MacKenzie, "Abuse-free optimistic contract signing," in *Proc. Adv. Cryptol.-CRYPTO 19th Annu. Int. Cryptol. Conf.* Santa Barbara, CA, USA. Cham, Switzerland: Springer, Aug. 1999, pp. 449–466.

[21] R. Chadha, M. Kanovich, and A. Scedrov, "Inductive methods and contract-signing protocols," in *Proc. 8th ACM Conf. Comput. Commun. Secur.*, Nov. 2001, pp. 176–185.

[22] N. Asokan, V. Shoup, and M. Waidner, "Asynchronous protocols for optimistic fair exchange," in *Proc. IEEE Symp. Secur. Privacy*, May 1998, pp. 86–99.

[23] J. L. Ferrer-Gomila, M. Payeras-Capella, and L. Huguet-Rotger, "Optimality in asynchronous contract signing protocols," in *Proc. Int. Conf. Trust, Privacy Secur. Digit. Bus.* Cham, Switzerland: Springer, 2004, pp. 200–208.

[24] G. Wang, "Generic non-repudiation protocols supporting transparent off-line TTP," *J. Comput. Secur.*, vol. 14, no. 5, pp. 441–467, Nov. 2006.

[25] H. Tian, J. He, and L. Fu, "Contract coin: Toward practical contract signing on blockchain," in *Proc. Int. Conf. Inf. Secur. Pract. Exper.* Cham, Switzerland: Springer, 2017, pp. 43–61.

[26] J.-L. Ferrer-Gomila, M. F. Hinarejos, and A.-P. Isern-Deyà, "A fair contract signing protocol with blockchain support," *Electron. Commerce Res. Appl.*, vol. 36, Jul. 2019, Art. no. 100869.

[27] H. Huang, K. Li, and X. Chen, "Blockchain-based fair three-party contract signing protocol for fog computing," *Concurrency Comput., Pract. Exper.*, vol. 31, no. 22, Nov. 2019, Art. no. e4469.

[28] L. Zhang, H. Zhang, J. Yu, and H. Xian, "Blockchain-based two-party fair contract signing scheme," *Inf. Sci.*, vol. 535, pp. 142–155, Oct. 2020. [Online]. Available: https://www.sciencedirect.com/science/article/pii/S0020025520304631

[29] J.-L. Ferrer-Gomila and M. F. Hinarejos, "A multi-party contract signing solution based on blockchain," *Electronics*, vol. 10, no. 12, p. 1457, Jun. 2021. [Online]. Available: https://www.mdpi.com/2079-9292/10/12/1457

[30] T. Zhang, Y. Wang, Y. Ding, Q. Wu, H. Liang, and H. Wang, "Multi-party electronic contract signing protocol based on blockchain," *IEICE Trans. Inf. Syst.*, no. 2, pp. 264–271, 2022.

[31] S. Han and X. Zhu, "Blockchain based spectrum sharing algorithm," in *Proc. IEEE 19th Int. Conf. Commun. Technol. (ICCT)*, Oct. 2019, pp. 936–940.

[32] H. Alhosani, M. H. U. Rehman, K. Salah, C. Lima, and D. Svetinovic, "Blockchain-based solution for multiple operator spectrum sharing (MOSS) in 5G networks," in *Proc. IEEE Globecom Workshops (GC Wkshps*, Dec. 2020, pp. 1–6.

[33] P. Lin, J. Jia, Q. Zhang, and M. Hamdi, "Dynamic spectrum sharing with multiple primary and secondary users," in *Proc. IEEE Int. Conf. Commun.*, May 2010, pp. 1–5.

[34] Z. Li, W. Wang, Q. Wu, and X. Wang, "Multi-operator dynamic spectrum sharing for wireless communications: A consortium blockchain enabled framework," *IEEE Trans. Cognit. Commun. Netw.*, vol. 9, no. 1, pp. 3–15, Feb. 2023.

[35] J. Qiu, D. Grace, G. Ding, J. Yao, and Q. Wu, "Blockchain-based secure spectrum trading for unmanned-aerial-vehicle-assisted cellular networks: An operator's perspective," *IEEE Internet Things J.*, vol. 7, no. 1, pp. 451–466, Jan. 2020.

[36] S. Jiang, X. Li, and J. Wu, "Multi-leader multi-follower Stackelberg game in mobile blockchain mining," *IEEE Trans. Mobile Comput.*, vol. 21, no. 6, pp. 2058–2071, Jun. 2022.

[37] C. Xu, K. Zhu, C. Yi, and R. Wang, "Data pricing for blockchain-based car sharing: A Stackelberg game approach," in *Proc. GLOBECOM IEEE Global Commun. Conf.*, Dec. 2020, pp. 1–5.

[38] G. Interdonato, E. Björnson, H. Quoc Ngo, P. Frenger, and E. G. Larsson, "Ubiquitous cell-free massive MIMO communications," *EURASIP J. Wireless Commun. Netw.*, vol. 2019, no. 1, pp. 1–13, Dec. 2019.

[39] Z. Han, D. Niyato, W. Saad, and T. Başar, *Game Theory for Next Generation Wireless and Communication Networks: Modeling, Analysis, and Design*. Cambridge, U.K.: Cambridge Univ. Press, 2019.

[40] D. Yaga, P. Mell, N. Roby, and K. Scarfone, "Blockchain Technology Overview," Jun. 2019, *arXiv:1906.11078*.

[41] S. Haghighatshoar and G. Caire, "Massive MIMO pilot decontamination and channel interpolation via wideband sparse channel estimation," *IEEE Trans. Wireless Commun.*, vol. 16, no. 12, pp. 8316–8332, Dec. 2017.

[42] D. Neumann, M. Joham, and W. Utschick, "Covariance matrix estimation in massive MIMO," *IEEE Signal Process. Lett.*, vol. 25, no. 6, pp. 863–867, Jun. 2018.

[43] K. Upadhya and S. A. Vorobyov, "Covariance matrix estimation for massive MIMO," *IEEE Signal Process. Lett.*, vol. 25, no. 4, pp. 546–550, Apr. 2018.

[44] L. Sanguinetti, E. Björnson, and J. Hoydis, "Toward massive MIMO 2.0: Understanding spatial correlation, interference suppression, and pilot contamination," *IEEE Trans. Commun.*, vol. 68, no. 1, pp. 232–257, Jan. 2020.

[45] D. Fudenberg and J. Tirole, *Game Theory*. Cambridge, MA, USA: MIT Press, 1991.

[46] R. G. Gallager, *Information Theory and Reliable Communication*, vol. 2. Cham, Switzerland: Springer, 1968.

[47] L. Lamport, R. Shostak, and M. Pease, "The byzantine generals problem," *ACM Trans. Program. Lang. Syst.*, vol. 4, no. 3, pp. 382–401, Jul. 1982, doi: 10.1145/357172.357176.

[48] G. Wood, "Ethereum: A secure decentralised generalised transaction ledger," *Ethereum Project Yellow Paper*, vol. 151, pp. 1–32, Apr. 2014.

[49] Ethereum.org. (2024). *Smart Contracts Languages*. Accessed: Apr. 1, 2024. [Online]. Available: https://ethereum.org/en/developers/docs/smart-contracts/languages/
[50] Nomic Foundation. (2024). *Ethereum Development Environment for Professionals*. Accessed: Apr. 1, 2024. [Online]. Available: https://hardhat.org
[51] Etherscan. (2024). *Block Explorer and Analytics Platform for Ethereum*. Accessed: Apr. 1, 2024. [Online]. Available: https://etherscan.io/
[52] Polygonscan. (2024). *Block Explorer and Analytics Platform for Polygon*. Accessed: Apr. 1, 2024. [Online]. Available: https://polygonscan.com/gastracker

GUILLEM FEMENIAS (Senior Member, IEEE) received the Telecommunication Engineering and Ph.D. degrees in electrical engineering from the Technical University of Catalonia (UPC), Barcelona, Spain, in 1987 and 1991, respectively.

From 1987 to 1994, he was a Researcher with UPC, where he became an Associate Professor, in 1992. In 1995, he joined the Department of Mathematics and Informatics, University of the Balearic Islands (UIB), Spain, where he became a Full Professor, in 2010. He is currently leading the Mobile Communications Group, UIB, where he has been the Project Manager of numerous projects funded by the Spanish and Balearic Islands Governments. In the past, he was also involved with several European projects. His current research interests and activities include digital communications theory and wireless communication systems, with a particular emphasis on radio resource management strategies applied to 5G and 6G wireless networks. On these topics, he has published more than 100 journal and conference papers and some book chapters.

Dr. Femenias has served for various IEEE conferences as a technical program committee member and a Local Organizing Committee Member for the IEEE Statistical Signal Processing (SSP 2016). He was a recipient of the Best Paper Awards from the 2007 IFIP International Conference on Personal Wireless Communications and the 2009 IEEE Vehicular Technology Conference-Spring. He served as the Publications Chair for the IEEE 69th Vehicular Technology Conference (VTC-Spring 2009).

M. FRANCISCA HINAREJOS received the M.S. degree in telecommunication engineering, in 2003, and the Ph.D. degree in computer science from the Technical University of Catalonia, in 2010. She is currently an Assistant Professor with the Department of Computer Science, University of the Balearic Islands. She has authored several papers published in national and international conferences and international journals. Her research interests include network security, electronic commerce, security in constrained environments, cybersecurity, and blockchain. She leads national projects in these areas.

FELIP RIERA-PALOU (Senior Member, IEEE) received the B.S./M.S. degree in computer engineering from the University of the Balearic Islands (UIB), Mallorca, Spain, in 1997, the M.Sc. and Ph.D. degrees in communication engineering from the University of Bradford, U.K., in 1998 and 2002, respectively, and the M.Sc. degree in statistics from The University of Sheffield, U.K., in 2006.

From May 2002 to March 2005, he was with Philips Research Laboratories, Eindhoven, The Netherlands, first as a Marie Curie Postdoctoral Fellow (European Union) and later as a Member of Technical Staff. While at Philips, he worked on research programs related to wideband speech/audio compression and speech enhancement for mobile telephony. From April 2005 to December 2009, he was a Research Associate (Ramón y Cajal Program, Spanish Ministry of Science) with the Mobile Communications Group, Department of Mathematics and Informatics, UIB. Since January 2010, he has been an Associate Research Professor (I3 Program, Spanish Ministry of Education) with UIB. His current research interests include signal processing and wireless communications.

JOSEP-LLUIS FERRER-GOMILA received the M.S. degree in telecommunications engineering from the Technical University of Catalonia, in 1991, and the Ph.D. degree in computer science from the University of the Balearic Islands, in 1998. He is currently an Associate Professor with the Computer Science Department, University of the Balearic Islands. He has authored several papers published in national and international conferences and international journals. His research interests include network security and electronic commerce. He leads national projects in these areas.

AMADOR JAUME-BARCELÓ received the M.S. degree in telecommunication engineering from the University of the Balearic Islands, in 2021. He is currently a Research Assistant with the Computer Science Department, University of the Balearic Islands. His research interests include cybersecurity and blockchain.